






Development and Anatomy of the Human Middle Ear

4

Charlotte M. Burford , Hannah L. Cornwall ,
Matthew R. B. Farr , Claudia M. Santoni ,
and Matthew J. Mason 

Introduction

Contained within the temporal bone of the skull, the human middle ear (Fig. 4.1) comprises a system of air-filled cavities, communicating with the nasopharynx via the Eustachian tube (ET). The tympanic membrane, which separates the external meatus from the middle ear cavity, is connected to the malleus, the first of the three auditory ossicles that cross the cavity to communicate acoustic vibrations through to the inner ear. Two small muscles insert on these ossicles, and several nerves and arteries pass through or near the middle ear region. The embryology and adult anatomy of this region is complex and is often covered only briefly in textbooks and undergraduate medical courses. However, a knowledge of the structural relationships between the middle ear components and how they come to develop is essential for understanding the function of the middle ear and necessary for the provision of safe surgical care. In this chapter, we shall first review middle ear development before providing an overview of adult anatomy.

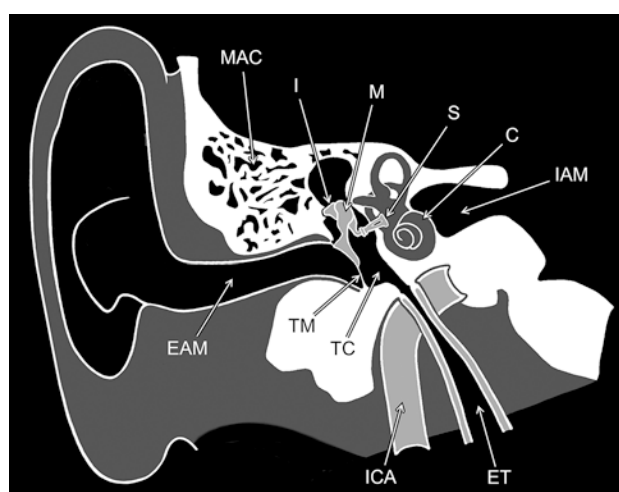


Fig. 4.1 Diagrammatic representation of the human peripheral auditory system (right ear, anterior view). *C*, cochlea; *EAM*, external auditory meatus; *ET*, Eustachian tube; *I*, incus; *IAM*, internal auditory meatus; *ICA*, internal carotid artery; *M*, malleus; *MAC*, mastoid air cells; *S*, stapes; *TC*, tympanic cavity; *TM*, tympanic membrane

C. M. Burford
East Kent Hospitals University NHS Foundation Trust,
Ashford, Kent, UK
e-mail: charlotte.burford1@nhs.net

H. L. Cornwall
Department of Paediatrics, Ysbyty Gwynedd, Bangor, Wales, UK

M. R. B. Farr
Doncaster Royal Infirmary, Doncaster, S Yorks, UK

C. M. Santoni
School of Clinical Medicine, University of Cambridge,
Cambridge, Cambridgeshire, UK
e-mail: cms208@cantab.ac.uk

M. J. Mason (✉)
Department of Physiology, Development & Neuroscience,
University of Cambridge, Cambridge, Cambridgeshire, UK
e-mail: mjm68@cam.ac.uk

Part 1: Development of the Middle Ear

Many of the structures in the head and neck, including the middle ear, arise from the pharyngeal apparatus of the embryo (Fig. 4.2). The development of the pharyngeal apparatus and its derivatives has been extensively studied in humans and model organisms [1, 2]. In humans, this apparatus consists of five pairs of arches (I–IV and VI), which form on either side of the developing foregut. Although it is sometimes said that arch V appears transiently but then regresses, it has recently been argued that it does not exist at all in amniotes and the other arches should be renumbered accordingly [3]. The arches appear between the second and fourth weeks of gestation [4]. Externally, the pharyngeal arches are covered with ectoderm, which invaginates to form pharynx

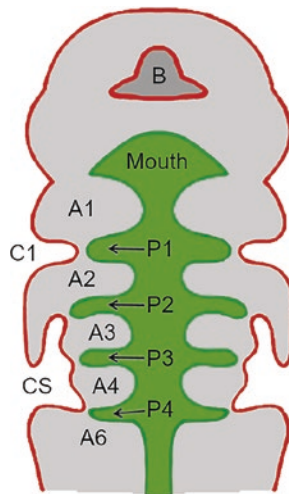


Fig. 4.2 Schematic representation of the pharyngeal apparatus in the early human embryo, demonstrating the contribution of the three germ cell layers (ectoderm = red; mesoderm = grey; endoderm = green). *A1–6*, pharyngeal arches I–VI (there is no arch V); *B*, developing brain; *C1*, pharyngeal cleft I; *CS*, cervical sinus; *P1–4*, pharyngeal pouches I–IV

geal clefts. In humans, there is one distinct cleft (I) between arches I and II, whereas a cavity called the cervical sinus represents the combined equivalent of clefts II, III and IV [1]. Internally, the endodermal lining invaginates to form pharyngeal pouches. As the clefts and pouches extend towards one another, they separate the intervening tissue into individual pharyngeal arches.

The mesodermal core of the pharyngeal arches is surrounded by mesenchyme arising from the neural crest, the cells of which migrate from the nearby regions on the dorsal surface of the developing neural tube. The mesodermal core gives rise to the skeletal muscles, whereas the neural crest-derived cells give rise to bony and cartilaginous structures, including the ossicles. The arches are innervated by particular cranial nerves, for example V_3 to the first arch and VII to the second: this has been used to establish muscle origins. The pharyngeal arches grow at differing rates during embryogenesis, leading to arches I and II becoming larger in volume than the others. These two arches and their intervening structures will form the components of the external and middle ears, discussed in more detail in the following sections.

Congenital abnormalities of pharyngeal arch development are well-documented in the literature. They can include complete fistulae arising from the first or second pharyngeal cleft and pouch contact, persisting into postnatal life [5].

The Middle Ear Cavity

Using the chick as a model of ear development, studies have shown that the endodermal cells of the pharyngeal pouches contain a web of actin fibres, just underneath their apical

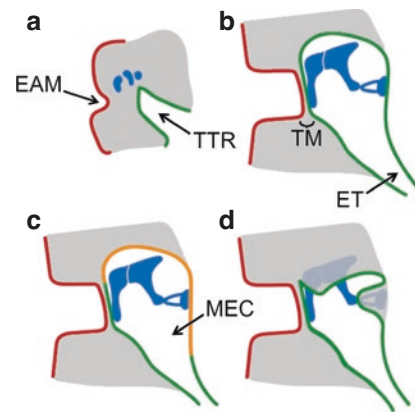


Fig. 4.3 Development of the middle ear cavity. (a) Middle ear ossicles condensing between the developing external auditory meatus and the tubotympanic recess. (b) The ‘endodermal model’ in which the epithelium covering the middle ear cavity is entirely endodermal in origin. (c) The ‘mesenchymal model’ in which the epithelium of the dorsal wall and the majority of the lateral wall of the middle ear cavity is mesenchymal in origin, whereas the medial and ventral walls are endodermal. (d) Schematic representation of the findings of van Waegeningh et al. [7] in a 25-week fetus, which these authors argue support the ‘endodermal model’. They demonstrated cavitation to the level of the ossicles, with the loose connective tissue remaining in the attic, and a continuous epithelium. Both models agree that the tympanic membrane is composed of thin layers of ectoderm, endoderm and mesoderm. *EAM*, external auditory meatus; *ET*, Eustachian tube; *MEC*, middle ear cavity; *TM*, tympanic membrane; *TTR*, tubotympanic recess. Red = ectoderm; green = endoderm; grey = mesoderm; blue = auditory ossicles; orange = middle ear cavity lining that has undergone a mesenchymal-to-epithelial transition

plasma membranes, which appear to constrain pouch morphology and direct their expansion [6]. The first pharyngeal pouch in humans begins to expand outwards in the fourth week of gestation [4]. It forms the tubotympanic recess, a wing-like evagination of the pharynx, which will ultimately form the middle ear cavity and Eustachian tube (ET; Figs. 4.3a and 4.4). The second pharyngeal pouch may contribute to the posterior part of the recess, at least initially [8–10]. The recess reaches the middle ear region at around 8 weeks of gestation and reaches the antrum by 29 weeks [11].

The middle ear region is originally entirely cellular in the embryo. As it develops, an epithelium-lined cavity forms, filled with fluid in utero, which contains the auditory ossicles and the inserting tendons of the two middle ear muscles. This process by which the mesenchymal cells surrounding the ossicles and developing muscle tendons are cleared is referred to as ‘cavitation’. In humans, cavitation begins in the third month and is normally complete prior to birth [12], although residual mesenchyme is frequently found in both children and adults (see later).

How exactly cavitation happens is linked to the origins of the epithelial lining of the middle ear cavity. There are two main theories describing the origins of the middle ear cavity epithelium: the ‘endodermal model’ and the ‘mesenchymal model’ [13]. The endodermal model, originally proposed by

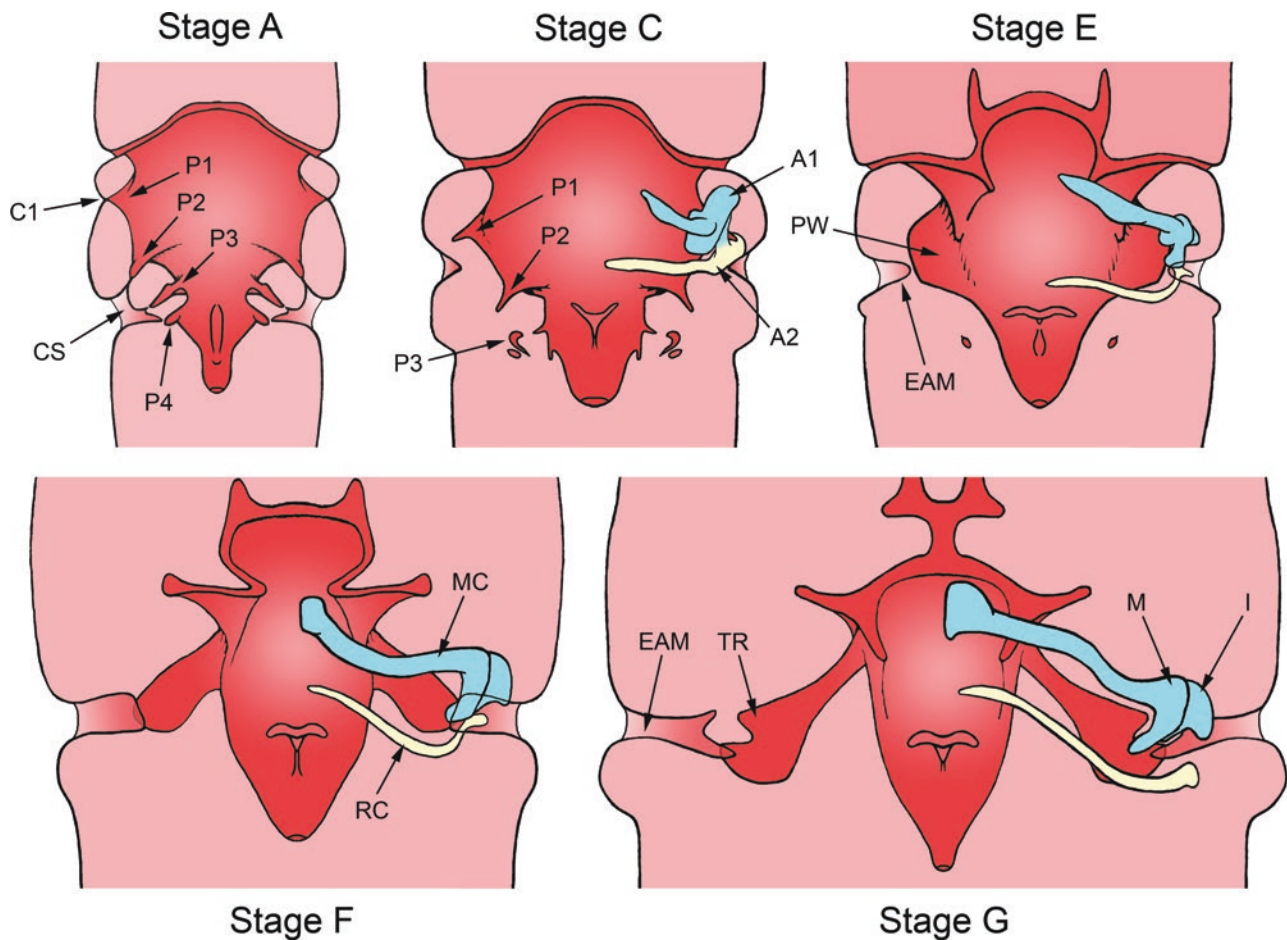


Fig. 4.4 Diagrammatic rostral views of five stages of pharyngeal development in human embryos, based on WinSurf reconstructions; not to scale. The pharynxes are curved in these embryos: each opens into the oral and nasal cavities towards the top of the diagram, while at the bottom, it tapers into the oesophagus. Derivatives of the first pharyngeal arch mesenchyme are colour-coded blue, derivatives of second pharyngeal arch mesenchyme cream. These are shown, where apparent, on each embryo's left side only. The first and second pharyngeal arch mesenchyme is beginning to condense into ossicular precursors in stage C; just in front of the first pouch, the two mesenchymal populations cannot be separated. The developing stapes is hidden behind the first pouch and first-arch derivatives, and hence is not visible in the figures. The original contact between pouch I and the caudodorsal end of pharyngeal

cleft I is visible in the stage A embryo but later disappears. The external auditory meatus develops as a separate invagination from the rostroventral end of cleft I. (Reprinted with the permission of John Wiley & Sons, Inc. from Burford, C.M. & Mason, M.J. (2016) Early development of the malleus and incus in humans. *Journal of Anatomy* 229:857–870. ©2016 Anatomical Society). Key: A1–2 mesenchymal condensations within pharyngeal arches I–II; C1 pharyngeal cleft I; CS lateral cervical sinus from which pharyngeal clefts II–IV originate; EAM external auditory meatus; I incus; M malleus; MC Meckel's cartilage; PW pharyngeal 'wing' (precursor of tubotympanic recess); P1–4 pharyngeal pouches I–IV; RC Reichert's cartilage; TR tubotympanic recess. Stage A, 7–9 mm crown-rump length (CRL); Stage C, 10–15 mm CRL; Stage E, 14–18 mm CRL; Stage F, 20–22 mm CRL; Stage G, 24–28 mm CRL

Wittmaack [14], states that the expanding tubotympanic recess invades the middle ear region and envelopes the developing middle ear structures. In this model, the entire middle ear cavity is lined with an epithelium which is wholly endodermal in origin (Fig. 4.3b). How the endoderm might come to enwrap the ossicles is unclear, but it might potentially rupture at some point, continue to migrate around the cavity and later reunite to create a complete lining [13]. The mesenchymal model was first proposed by Schwarzbart [15] after histological examination of more than 100 human temporal regions, aged from four fetal months to adulthood. According

to this model, the endoderm of the tubotympanic recess ruptures and the lining of much of the middle ear cavity is instead formed from the mesenchyme, which migrates and retracts to the edges of the cavities (Fig. 4.3c).

These competing theories were put to the test by Thompson and Tucker [16]. Immunostaining for E-cadherin in a mouse model showed that the intact endodermal lining of the first pharyngeal pouch on embryonic day 15.5 breaks down to allow an influx of mesenchyme by day 17.5. Transgenic mouse lines were used to investigate the origin of the cells ultimately lining the middle ear cavity: *Sox17-*

2*AicreR26R* reporter lines for tissues with endodermal origins and *Wnt1creR26R* for neural crest-derived cells. Thompson and Tucker found that the epithelium covering the dorsal wall of the mouse middle ear cavity, and the majority of the medial wall including the cochlear promontory, originates from neural crest mesenchyme, whereas that covering the medial side of the tympanic membrane, much of the ventral wall and the Eustachian tube is endodermal. In addition, they studied the expression of the epithelial-specific protein cytokeratin 14 and demonstrated that this protein was expressed in the neural crest-derived region between postnatal days 14 and 16. This mesenchymal-to-epithelial transition occurred concomitant with the formation of the final middle ear cavity. Retraction of mesenchyme consistent with this model has also been observed in shrew and opossum, suggesting that it is widespread among mammals [13].

Thompson and Tucker [16] found that the component of the lining of the mouse middle ear cavity derived from endoderm was ciliated and contained mucus-secreting goblet cells, whereas the part derived from mesenchyme was a simple, non-ciliated epithelium. In humans, the lining of the Eustachian tube, anterior tympanic cavity and hypotympanum are ciliated, with goblet cells around the ET region, whereas the epitympanum, antrum and mastoid are covered with a squamous epithelium, which normally shows very few cilia [17–19]. The similar histological pattern between mice and humans is consistent with a similar dual origin of the middle ear epithelium in humans.

However, the ‘mesenchymal model’ of the human middle ear cavity epithelium is not universally supported. van Waegeningh et al. [7] carefully examined the epithelial lining of the middle ear cavity using immunohistological sections from one 25-week gestation fetus. The process of cavitation had only just passed the level of the ossicles in their specimen, as the loose mesenchyme remained around the attic. Significantly, the whole cavitated region was covered by an intact epithelium, which, these authors argued, could represent endoderm, which had expanded to enwrap the ossicles without rupturing (Fig. 4.3d).

Irrespective of whether the epithelium of the human middle ear is derived entirely from endoderm, or from both endoderm and mesenchyme, the mesenchyme that fills the middle ear cavity prenatally must somehow be replaced with fluid and, later, air. Based on observations and measurements made from postnatal human temporal bones, Piza et al. [20, 21] suggest that the mesenchyme recedes as the middle ear cavity expands, thinning as it does so and thus contributing to the submucosal lining of the cavity, from which it is not easily distinguished. Other studies suggest that mesenchymal cells disintegrate. Terminal deoxynucleotidyl transferase dUTP nick end labelling (TUNEL) assays, which detect DNA fragmentation, have been used to demonstrate apoptosis of the middle ear mesenchyme, thus contributing to cavi-

tation in rodents, from the 16th embryonic day until after birth in rats [22] but only on postnatal day 1 in mice [23]. Degenerating mesenchymal cells were also observed in human temporal bones, postnatally [24]. The association between retained mesenchyme in the middle ear cavity and otitis media is discussed later.

The Tympanic Membrane and the External Auditory Meatus (EAM)

The tympanic membrane is made up of three layers (Fig. 4.3). The outermost layer is an invagination of the ectodermal lining of the external auditory meatus, whereas the inner layer consists of the middle ear cavity lining, which the studies mentioned above agree would be endodermal in origin at this location. Fibrous mesenchyme forms a middle layer between the outer and inner layers. It is often, although mistakenly, believed that the tympanic membrane forms where the first pharyngeal cleft meets the first pharyngeal pouch. However, the primitive connection between the first cleft and the first pouch is, in fact, lost [25], and a secondary connection forms between the true external auditory meatus (EAM) and the tubotympanic recess [8]. Mouse models of EAM development show the definitive EAM developing in mesenchyme, which is entirely *Hoxa2*-negative and therefore seemingly of first-arch origin only [26]. The plane of the tympanic membrane is nearly horizontal in the early human fetus, becoming more vertical throughout fetal life and also increasingly inflected at the umbo [27].

It was suggested that the formation of the middle ear cavity and tympanic membrane is coordinated by an ‘epidermoid formation’, identified at the primitive connection where pouch I meets cleft I [28, 29] and persisting in some specimens postnatally, at the junction between the middle ear and the ET epithelia, just anterior to the tympanic membrane [30]. Later molecular studies have focused instead on the role of the tympanic ring, which undergoes intramembranous ossification to provide a frame for the tympanic membrane and will go on to form part of the temporal bone (see later). Mouse molecular genetic investigations have strongly suggested that tympanic ring development is necessary for the invagination of the external meatus and for the development of the tympanic membrane [31]. For example, mice deficient in expression of *Gooseoid* (*Gsc*) fail to develop a tympanic ring, a tympanic membrane and an EAM and also have other craniofacial defects [32–34]. Defects, including bilateral EAM atresia, have been linked to the human syndrome SAMS (a syndrome of short stature, auditory canal atresia, mandibular hypoplasia and skeletal abnormalities), which is also caused by *Gsc* genetic mutations [35]. Experimental evidence in mice suggests that the development of the manubrium of the malleus, which is attached to

the interior surface of the tympanic membrane, depends on the normal development of the external meatus [36], and this appears to be the case in humans too [37]. In one study, 98% of those with severely defective external ear development were found to have ossicular dysplasias, and other middle ear defects were also commonly observed [38].

Eustachian Tube Development

The Eustachian tube (ET), named after the sixteenth century Italian anatomist Bartolomeo Eustachi (1500–1574) [39], is also known as the auditory tube or pharyngotympanic tube. Beginning as an expansion from the first pharyngeal pouch around the fourth week of gestation [4], the tube is transformed by epithelial differentiation and the development of cartilage and muscle from around the ninth week [40]. The development of the ET is of specific clinical interest due to its postulated links to pathologies such as otitis media [41–43].

The cartilage of the ET develops between about the 12th and 20th weeks of gestation, beginning at the pharyngeal end and progressing towards the middle ear [40]. The tube increases in length throughout gestation [40], with the main period of extension of the cartilaginous part occurring between weeks 16 and 28 [44]. Mouse models have shown that most of the ET cartilage is mesodermal in origin, but there is a small, dorsal component derived from the neural crest [45]. The bony portion of the Eustachian tube undergoes upward expansion in the late fetal stage, and this continues through childhood, thus contributing to the supratubal recess [46]. The lumen of the tube begins as round in cross section, becoming oval, and then, from around the 27th week, slit-shaped [40], but it is said to remain patent throughout prenatal life [47].

In neonates, the ET has a narrower diameter than in adults, especially the cartilaginous region [48, 49]. A child's ET has a rather uniform cross section along much of its length, whereas in an adult, it is more gradually tapering from a large pharyngeal orifice towards the narrowest portion, which is near the tympanic end of the cartilaginous zone [50]. The tube is also shorter in absolute length in children, with a relatively shorter bony section, and it is straighter than that of adults [51]. At 6 months' gestation, the ET is horizontal; by 6 months of age, it forms an angle of around 10° to the skull base [52]. Although the ET is shorter and more horizontally inclined in children under the ages of around 7, compared to adults, the fact that older children are more similar in these respects to adults, and that no difference was found between children with and without otitis media, suggests that the length and inclination of the tube may not contribute to susceptibility to this disease [53]. Other studies, however, have suggested that such a link might exist [54].

Muscles of the Eustachian Tube

Derived from the first pharyngeal arch, the tensor veli palatini (TVP) is first seen around week 6 in the human embryo, arising with the medial blastema of the muscles of mastication, together with the medial pterygoid and tensor tympani muscles [55]. All were found to be innervated by the medial root of the mandibular nerve (V). By week 7, the TVP is differentiated and related to the pterygoid hamulus, and it becomes continuous with the palatine aponeurosis by week 9. At week 13, there is a connective tissue link between the TVP and the goniale of the malleus. By birth the TVP has reached its adult relationship with the ET mesenchyme at one end, and at the other end with the palatine aponeurosis. The pterygoid hamulus, around which the TVP tendon glides, chondrifies around week 8 [55] and ossifies around week 16 [40]. The TVP remains in mesenchymal and later tendinous connection with the tensor tympani muscle throughout its development [56].

The levator veli palatini (LVP) is first seen around week 8, just ventromedial to the pharyngeal aperture of the ET; by week 9, it is found to run along the full length of the ET [57]. Kishimoto et al. found the LVP to receive innervation from the lesser palatine nerve, a branch of VII. Although innervated via the pharyngeal plexus [58] and classically believed to derive from pharyngeal arches IV–VI, Kishimoto et al. [57] suggest that the LVP may actually originate from pharyngeal arch II, based on its anatomical relationship with the ET and the component of its innervation from the facial nerve. Both *Tbx1*^{+/-} and *Df1*^{+/+} mice, used as models of DiGeorge syndrome in humans, were found to have smaller LVP muscles than wild-type mice, and this was associated with an increased incidence of otitis media [59].

Very little is known about the development of the salpingopharyngeus muscle. It is closely associated with the other longitudinal pharyngeal muscles, representing part of the palatopharyngeus complex [60, 61]. As such, its innervation and pharyngeal arch origin are probably similar to those of the LVP. The salpingopharyngeus muscle was not found to be present by week 8 of development [62].

Middle Ear Ossicle Development

The three middle ear ossicles, found in all mammals, are the malleus, incus and stapes. These are the Latin terms for a hammer, anvil and stirrup, respectively, reflecting their shape.

The pharyngeal arch origins of the ossicles have been much debated [63, 64]. The currently favoured theory, initially proposed by Reichert [65], states that the malleus and incus develop from the caudal end of Meckel's cartilage, which arises within pharyngeal arch I, whereas the stapes develops from the cartilage of pharyngeal arch II (Reichert's

cartilage: Figs. 4.4 and 4.5). Meckel's cartilage, a long rod which forms the lower jaw in embryonic life, separates from the malleus during later development [66]. The anterior process of the malleus develops as a separate, intramembranous ossification referred to in the embryo as the goniale [67–69].

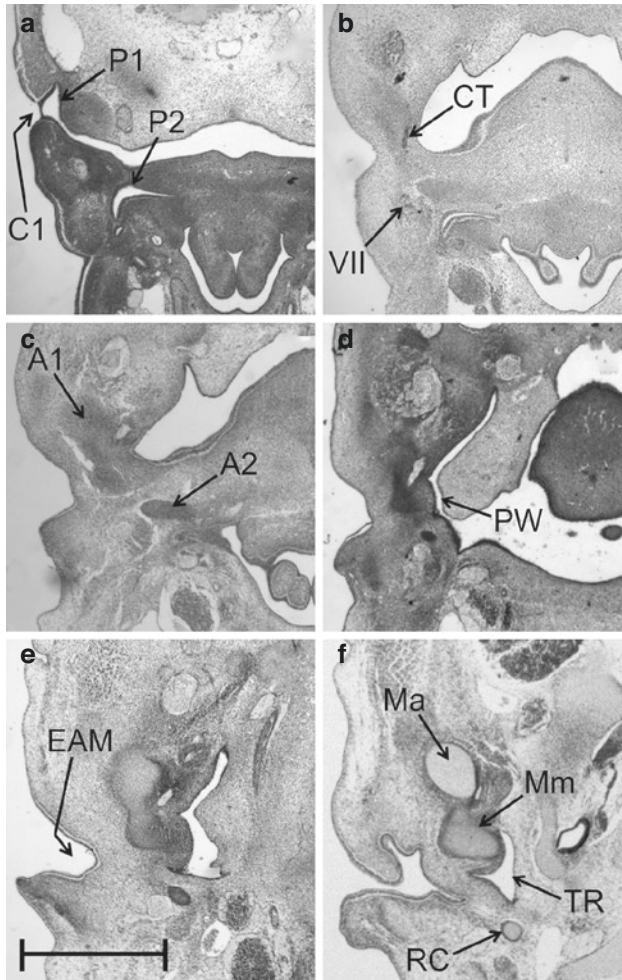


Fig. 4.5 Photomicrographs of sections through the left ear region of six human embryos, between around 5.5 and 8 weeks of gestation, from the Boyd Collection, University of Cambridge. (a) 9.5-mm crown-rump length (CRL); (b) 13.5-mm CRL; (c) 14.5-mm CRL; (d) 17 mm-CRL; (e) 20-mm CRL; (f) 24-mm CRL. In the early embryo, the first pharyngeal pouch meets the first cleft, visible in panel (a), but this transient spiracular union soon disappears. Sections b–f are rostroventral to this, where the true external auditory meatus is developing. In panel (b), the incipient meatus is visible as the indentation to the left of the chorda tympani nerve. The meatus converges on the extension of the pharynx that will become the tubotympanic recess, leaving the manubrium of the malleus sandwiched in between (c–f). The tissue between the meatus and recess will continue to narrow and the tympanic membrane will develop here. A1, A2, mesenchyme condensing in pharyngeal arches I and II, respectively; C1, pharyngeal cleft I; CT, chorda tympani nerve; EAM, external auditory meatus; Ma, body of the malleus; Mm, manubrium of the malleus; P1, P2, pharyngeal pouches I and II, respectively; PW, pharyngeal ‘wing’ (precursor of the tubotympanic recess); RC, Reichert’s cartilage; TR, tubotympanic recess; VII, facial nerve. Scale bar for all photomicrographs = 1 mm

The view that the bulk of the malleus and all of the incus are derived from pharyngeal arch I has been supported by more recent evidence from mouse genetic models. Mice with homozygous mutations in *Hoxa2*, a gene expressed in arch II which is known to play a role in early embryonic facial development, show duplication of first-arch structures, including the malleus and incus, but lack a stapes [70, 71].

However, others have argued for a ‘dual-arch’ origin of the malleus and incus in humans, claiming that whilst the bodies of the incus and malleus are derived from the first pharyngeal arch, the manubrium of the malleus and the long process of the incus are actually second-arch structures. The earliest evidence supporting this theory comes from Hanson et al. [72], who examined human embryonic specimens between approximately 6 and 9.5 weeks of gestational age. They described the primitive blastemal mass, which will later form the malleus and incus, extending across the first pharyngeal cleft into the second pharyngeal arch region. Tracing the development of this blastemal mass suggested that the manubrium of the malleus and the long process of the incus actually developed from the region of pharyngeal arch II. This finding was corroborated by Louryan [73], who independently examined embryonic specimens of a similar age. Whyte et al. [74] also supported the dual-arch origin theory but described the long process and the manubrium fusing with the ossicular bodies at a later stage, around 9.5 weeks in their series. Further support for this theory came from observations that the stapedius muscle tendon can have a small insertion onto the long process of the incus as well as the stapes [72, 75], the stapedius being of second-arch origin. This ‘dual-arch’ theory was presented in the form of a figure in the 37th, 38th and 39th editions of *Gray’s Anatomy* [76–78].

More recent histological examinations of human embryonic specimens have failed to find any clear evidence to support the dual-arch hypothesis [8, 79]. In mouse *Hoxa2* mutants, the long process of the incus was duplicated with the undisputed first-arch structures and was fused with its counterpart distally; the duplicated malleus shared one manubrium, which was longer than that in the wild-type [71]. O’Gorman [80] used lineage tracing to determine the second-arch contributions to the middle ear in mice. The manubrium was found to be only first arch, but O’Gorman did identify a short process near the manubrium of the malleus that was a second-arch derivative. Although this process was referred to as the ‘*processus brevis*’, an alternative term for the lateral process of the malleus, it was subsequently identified as the orbicular apophysis [81]. The orbicular apophysis is a process of the mouse malleus, which is not found in the human ossicle and which is not homologous with the human lateral process. Louryan et al. [82] showed that Hox-A2 immunostaining, for second-arch derivatives, labelled the orbicular apophysis and Reichert’s cartilage of

mice very strongly, as expected. However, the rest of the ossicular chain, including the stapes, picked up diffuse labeling. This result is difficult to interpret, but Louryan et al. argued that it keeps alive the possibility of a second-arch contribution to the malleus and incus bodies.

The stapes is believed to largely arise from the pharyngeal arch II cartilage. A contribution of the human otic capsule to the stapes footplate had been suggested, based on histological observation [72, 83], but this was denied by Rodríguez-Vázquez [84]. However, O’Gorman [80] found that the peripheral footplate and the annular ligament did not label as second-arch neural crest derivatives, in mice. These portions were later shown to be mesodermally derived [85]. Thompson et al. found that the neural crest component is necessary for the normal formation of the mesodermal component, and the oval window.

Ossicular Embryology in More Detail

The loose, mesodermal condensations representing the first signs of the malleus and incus appear at around 5.5 weeks of gestation [72]. The malleus becomes precartilaginous by the seventh week and separates from the incus [67]. It begins to ossify around 15–16 weeks and reaches its maximum size at around 17–21 weeks, after which point Meckel’s cartilage degenerates into fibrous tissues contributing to the anterior ligament. Meanwhile, the goniale appears at around 8.5 weeks and fuses with the rest of the malleus between around 18 and 21 weeks [11, 67].

Studies in rodents [86] and humans [8, 72, 87] suggest that the malleus and incus are part of a single mesenchymal condensation, with a joint forming between the two ossicles later. In humans, the articular cavity starts to form in the ninth week of gestation and the capsular ligament becomes visible in the following week [88]. In patients with Treacher Collins syndrome (TCS), the malleus and incus are often fused together, hypothesised to occur as the result of disruption to this joint formation process [89, 90]. A more recent study has suggested that the earliest trace of the incus forms independently of Meckel’s cartilage within the first arch, appearing as a separate mesenchymal condensation to that of the malleus at 6 weeks’ gestation and only joining the malleus shortly afterwards [79]. Rodríguez-Vázquez et al. [91] found that a transient cartilaginous union between what will become the short process of the incus and the otic capsule forms from week 8 onwards. Having passed through a stage where there is a narrow joint cavity between the short process and the otic capsule, laterally, the articulation becomes fully fibrous from 17 weeks onwards. The incus begins to ossify just before the malleus, at around 16 weeks [11, 92].

The incudostapedial joint starts as densely-packed mesenchyme between the distal long process and what will become the stapes head, at 7–8 weeks’ gestation [88]. The

lenticular apophysis of the incus forms at around 9 weeks, and the incipient incudostapedial joint cavity first appears at 13 weeks. The cavity is completed by around 16 weeks [88].

A variable amount of remodelling of both the malleus and incus occurs in postnatal life [67]. Yokoyama et al. [93] described bone marrow spaces persisting in the malleus and incus until 25 months of age, after which point they are replaced by narrow, vascular channels. Vestiges of embryonic cartilage have been described within the adult malleus and incus [94], and cartilage is found around the periphery of the manubrium [95] and lateral process [96]. The anterior process of the malleus appears to shorten slightly, postnatally [97].

The stapedial anlage, first visible at around 4.5 weeks’ gestation [72], begins as an ovoid, mesenchymal condensation, which is connected to Reichert’s cartilage through a separate condensation representing the interhyale [84]. The developing stapes is penetrated by the stapedial artery. This artery degenerates at around 7 weeks, during which time the stapes chondrifies, but the ossicle is left with its characteristic intercrural foramen [84]. Rarely, a stapedial artery passing through the stapes may persist through to adulthood in humans: variations in its morphology and its pharyngeal arch origins have been reviewed by Hitier et al. [98].

The developing stapes footplate is juxtaposed to the otic capsule by the end of the embryonic period, during which time the stapes takes the form of a bulky ring. The annular ligament begins as a mesenchymal condensation between the footplate and the otic capsule, visible at around 9 weeks, completing its differentiation into fibrous tissue by week 12 [88]. Stapes ossification begins at around 19 weeks [83]. Unlike the malleus and incus, which thicken over the course of prenatal development, the stapes undergoes considerable thinning. Attaining its maximum size at around 5 months’ gestation, it subsequently develops into a much more delicate ossicle with internally hollowed crura and a wider intercrural foramen, reaching near-adult morphology after around 7 months. However, the vestibular aspect of the footplate remains cartilaginous even in children [83].

Middle Ear Muscle Development

The two smallest skeletal muscles in the human body, the tensor tympani and stapedius, lie in the middle ear and insert on the malleus and stapes, respectively. The tensor tympani is derived from pharyngeal arch I and is hence innervated by the mandibular branch of the trigeminal nerve (V_3), whereas the stapedius is from arch II and is innervated by the stapedial branch of the facial nerve (VII).

The developing tensor tympani is already connected to the malleus at 6 weeks; its anlage is in communication with that of the tensor veli palatini via a mesenchymal connection

[56]. The *processus cochleariformis* develops at around 15–16 weeks' gestation [56]. Like the levator veli palatini, the tensor tympani was found to be smaller in heterozygous *Tbx1*^{+/-} mice than in wild-type [59].

The stapedius muscle develops from two initially separate parts. The tendon is derived from the interhyale, which develops as a mesenchymal condensation between the stapes and Reichert's cartilage around week 6 [84, 99]. The belly forms as a separate anlage, medial to the facial nerve, which joins with the interhyale around week 8; the external portion of the interhyale disappears by around 9 weeks, detaching the muscle and its tendon from Reichert's cartilage. The stapedius tendon is of variable length and angle in adults, which may depend on the position of attachment of the belly of the muscle to the interhyale during development [100]. The pyramidal eminence appears between 12 and 14 weeks [99].

Temporal Bone Development

The human temporal bone is a composite structure comprising petromastoid, styloid, tympanic and squamous components. It houses the bony external meatus, middle ear cavity and inner ear. The cartilaginous otic capsule, containing the inner ear, contributes to the petromastoid component of the temporal bone. It has been shown to be mesodermally derived in mice [85], except for a small component derived from second-arch neural crest [80]. The styloid process, which is joined to the otic capsule in the embryo, is derived from the cranial segment of Reichert's cartilage and so is of second-arch neural crest origin [85, 101]. The tympanic and squamous components of the temporal bone are also derived from the neural crest [102] but ossify directly in mesenchyme [91, 103].

From around 11 weeks' gestation, the tympanosquamous fissure begins to close and the tegmen tympani forms [104]. The tegmen tympani, which forms on the roof of the middle ear cavity, is considered part of the petromastoid component of the temporal bone. It initially forms as an independent cartilage, becoming almost fully ossified by 17 weeks [104]. The petromastoid, squamous and tympanic components of the temporal bone remain separate in the fetus, fusing only postnatally [105]. The development of the hypotympanum is considered in detail by Spector and Ge [106] and that of the facial recess and associated structures by Eby [107].

The Otic Capsule

The inner ear arises from the otic placode, a non-neural ectodermal thickening near the hindbrain region, associated with cranial nerve VIII [108, 109]. At 5–6 weeks, the otocyst, which will develop into the membranous labyrinth, is surrounded by mesenchyme, which has developed into the cartilaginous otic capsule by 8.5 weeks [108]. This becomes

increasingly complex in shape as the labyrinth develops within it. The otic capsule ossifies from a large number of separate centres, which first appear between around 16 and 21 weeks of gestation, and it reaches adult size in the fetus [11, 110]. The first signs of ossification in the otic capsule visible by computed tomography were seen at the age of 18.5 weeks [111].

The Tympanic Ring

The tympanic ring is an intramembranous ossification, developing from pharyngeal arch I [31]. Representing the border between the outer and middle ears, it contains a groove, the tympanic sulcus, to which the tympanic membrane attaches circumferentially. The tympanic ring appears as a distinct mesenchymal condensation in the eighth week of gestation [103]. It then begins to ossify without any cartilaginous precursor and increases in diameter. By 10 weeks, it is C-shaped, lying between Meckel's and Reichert's cartilages and lateral to a region which will later become the tympanic cavity. By 19 weeks, it forms an almost complete annulus but for a gap in its upper part known as the notch of Rivinus (*incisura tympanica*). Its rostral free end expands in the region of the anterior process of the malleus, where Meckel's cartilage begins to degenerate and the goniale fuses with the rest of the malleus [103].

Fetal tympanic rings are located below the auricle and are more horizontally inclined than they are in adults [112]. The ring nearly reaches adult diameter by around 34 weeks and begins to fuse with the otic capsule [103]. The orientation of the sulcus tympanicus, supporting the tympanic membrane, gradually becomes more vertical in later fetal and early postnatal life [27]. The ring remains open but is incorporated into the temporal bone near term [103]; lateral growth later leads to the formation of the bony external meatus [27, 113].

Molecular studies have found evidence of a role of the *Gsc* gene in condensation of the tympanic ring in the first-arch tissue: this fails in *Gsc*-null mice [114]. *Hoxa2* expression in pharyngeal arch II seems to inhibit the *Gsc*-expressing mesenchymal cells in that arch from developing a second tympanic ring [31].

The Mastoid

The small rodents most often used as model species in ear development studies lack cellular mastoid processes like those of humans [115], so what we know about mastoid development has had to come directly from observations on human specimens.

The connective tissue extending from the middle ear reaches the antral region at around 22 weeks' gestation; by 29 weeks, the epithelium of the tympanic cavity has arrived and begins to invade the diploic bone from there, resulting in the development of a cavity [116]. The future air cells begin

to extend outwards from the antral region into the mastoid before birth [116]. At birth, the antrum is well-pneumatised; most of the mastoid pneumatisation occurs from then until around 6 years of age, with continued expansion until the age of puberty, taking the air cells all the way to the petrous apex in some [117]. The possible pathways for the pneumatisation of the mastoid are illustrated by Halewyck et al. [118]. The overall extent of pneumatisation is highly variable between individuals, following a normal distribution [119]. The growth of the mastoid process of the temporal bone, which is largely independent of its internal excavation, occurs fastest in the first postnatal year but continues until puberty [117].

Mastoiditis in children may result in the formation of new bone and sclerosis, leading to failure of pneumatisation even after the infection is resolved; an infection can also obliterate pre-existing air cells [120].

Middle Ear Development and Otitis Media

Although it is generally held that the mesenchyme within the middle ear cavity should disappear within about a year of birth, its presence has been well-documented in some children and even in adults [12, 121, 122]. One study found mesenchyme in 2% of 1404 temporal bones of patients aged 5–81 years [123]. It has been suggested that this mesenchyme might block the aeration routes through to the rest of the middle ear cavity [122]. If this interferes with the drainage of exudate from the middle ear through the ET into the pharynx, then this may explain the association between retained mesenchyme in the middle ear and the development of otitis media [122–125]. Retained mesenchyme in the middle ear cavity has also been cited as a possible cause of conductive hearing loss in Down syndrome patients [126, 127]. Given this evidence, it has been suggested that cases of recurrent suppurative otitis media in young children could be better treated with tympanic paracentesis than with antibiotics [128]. Mesenchymal remnants may adversely affect the tympanic membrane and ossicular chain function and may also play a role in the formation of cholesteatoma [129].

Retained mesenchyme in the middle ear cavity seems to be most commonly found in the epitympanum/mastoid region [122, 123]. A poorly pneumatised mastoid is associated with a blocked tympanic isthmus [130], which may restrict aeration and drainage of the epitympanum and mastoid. This may help explain why underdevelopment of the mastoid air cells, a condition that has a hereditary element, is associated with more frequent presentations of acute otitis media [131]. However, what represents cause and what represents effect in these associations remains unclear.

Underdevelopment of the ET can result in fluid accumulating in the tympanic cavity, and this is considered to be an important cause of otitis media with effusion in children

[132]. It has been proposed that the evolution of larger brain volumes leading to the requirement for earlier birth in humans, alongside the flattening of the face and adaptations of the palate and its musculature associated with speech, may have reduced the functionality of the ET, predisposing humans to develop this condition [133]. As an experimental model of this condition, mice with mutations of *Eya4* have been found to have a narrower, malpositioned ET and inflammation of the middle ear cavity, and they also suffer from middle ear effusion and hearing loss [134].

Part 2: Anatomy of the Adult Middle Ear

The Tympanic Cavity

The Eustachian tube, tympanic cavity and mastoid complex (Fig. 4.6) are collectively described as the ‘middle ear cleft’. Of these, the tympanic cavity contains the key structures involved in sound transmission from the external to inner ears. The human tympanic cavity is commonly subdivided into three compartments. The epitympanum (epitympanic recess) contains the head of the malleus and the dorsal incus. It is separated from the mesotympanum below by the ossicles and the lateral incudal and tensor mucosal folds that surround them, but remains in communication with the mesotympanum by means of the narrow tympanic isthmus in the posteromedial quadrant [135]. The mesotympanum is

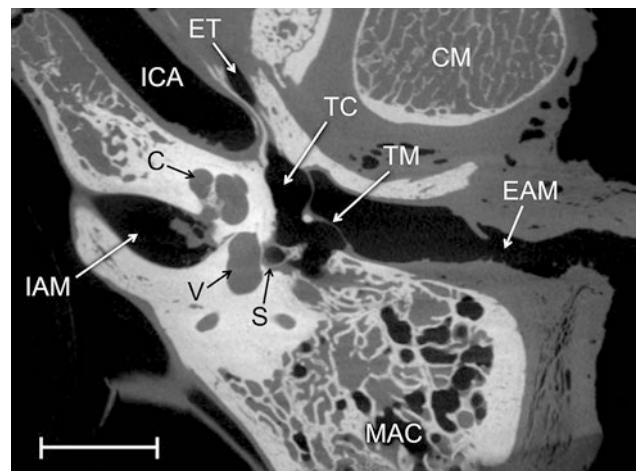


Fig. 4.6 Computed tomographic image of a preserved human temporal bone, in an approximately horizontal plane. The bone is white, the soft tissue and fluid are grey and air is black. The internal carotid artery and internal auditory meatus are both empty in this specimen but would not be in real life. *C*, cochlea; *CM*, condyle of the mandible; *EAM*, external auditory meatus; *ET*, Eustachian tube; *IAM*, internal auditory meatus; *ICA*, internal carotid artery; *MAC*, mastoid air cells, some of which are filled with fluid; *S*, stapes; *TC*, tympanic cavity; *TM*, tympanic membrane (the manubrium of the malleus is visible centrally); *V*, vestibule. Scale bar = 10 mm

that part of the middle ear cavity at the level of the tympanic membrane, and the hypotympanum is the region below the inferior extent of the tympanic sulcus.

The anterior wall of the tympanic cavity is superiorly comprised of the bony portion of the Eustachian tube, separated by a thin plate of bone from the tensor tympani muscle. Inferior to these structures runs the internal carotid artery (Fig. 4.6), which enters the temporal bone medial to the styloid process and initially runs vertically, anteroinferior to the cochlea. It then turns anteromedially and runs under the Eustachian tube towards the foramen lacerum, whence it enters the cranial fossa. Knowledge of the normal and aberrant courses of the carotid artery is essential for safe middle ear surgery.

The posterior wall of the middle ear cleft is penetrated superiorly by the *aditus ad antrum*, the opening that connects the epitympanum and the mastoid antrum (discussed later). Below the *aditus* is the pyramidal eminence, the bony prominence that contains the stapedius muscle belly; the tendon projects anteriorly and inserts on the stapes. The lower portion of the posterior wall of the tympanic cavity may be subdivided into two. ‘Facial recess’ is the term for the groove between the facial nerve and the tympanic annulus, whereas the *sinus tympani* is an extension of air cells into the posterior wall, deep to the facial nerve.

The bony medial wall of the tympanic cavity (Fig. 4.7) features the rounded elevation of the cochlear promontory, which is crossed by the tympanic branch of the glossopharyngeal nerve (IX). Posterosuperior to the promontory lies the oval window (*fenestra vestibuli*), which contains the stapes footplate held in place by the annular ligament. Inferior to this lies the round window niche, separated from the oval window by the subiculum. The round window niche is a small channel containing at its base the ‘secondary tympanic membrane’, which covers the round window itself, separating the middle ear cavity from the perilymph [136]. The round window (*fenestra cochleae*), accessed via a posterior tympanotomy into the facial recess from the mastoid antrum, is a common insertion point during cochlear implantation [137].

A large portion of cranial nerve VII, the facial nerve, runs in an anterior to posterior direction along the medial aspect of the tympanic cavity, prior to its descent through the mastoid. The nerve travels within the Fallopian canal, just superior to the oval window. The *processus cochleariformis*, a bony projection over which the tendon of the tensor tympani muscle runs, is a landmark for the anterior portion of the Fallopian canal. Posterosuperior to the Fallopian canal, the bone covering the lateral semicircular canal forms the medial part of the epitympanum.

The lateral boundary of the tympanic cavity consists of the tympanic membrane and bony walls of the epitympanum and hypotympanum, located superior and inferior to the

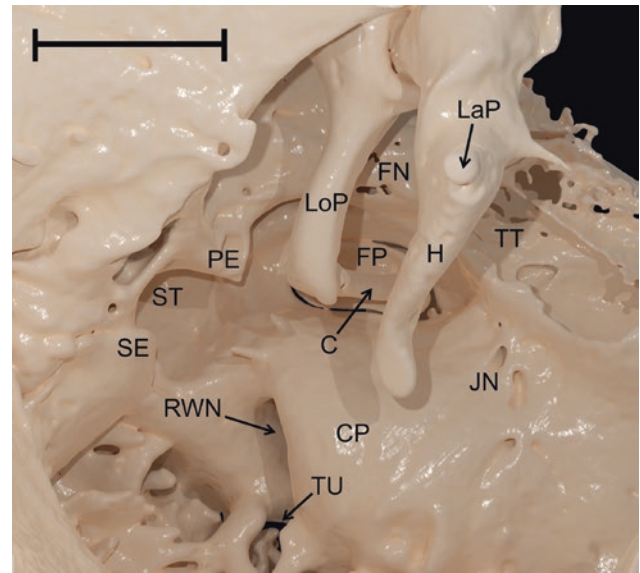


Fig. 4.7 Micro-CT reconstruction of the medial wall of the middle ear cleft, right ear. Scale bar = 3 mm. *C*, stapedial anterior crus; *CP*, cochlear promontory; *FN*, bony impression of the facial nerve; *FP*, footplate of stapes in the oval window; *H*, handle of the malleus (manubrium); *JN*, bony impression of Jacobson’s nerve; *LaP*, lateral process of the malleus; *LoP*, long process of the incus; *PE*, pyramidal eminence; *RWN*, round window niche; *SE*, styloid eminence; *ST*, sinus tympani, *TT*, bony canal of the tensor tympani muscle; *TU*, subcochlear tunnel

membrane, respectively. The wedge-shaped bony lateral wall of the epitympanum, termed the ‘scutum’, may be eroded by cholesteatoma.

The Tympanic Membrane

The tympanic membrane separates the external auditory meatus from the tympanic cavity (Fig. 4.6). In adults, this is a thin membrane about 9–10 mm in diameter, attached around its circumference to the sulcus of the tympanic bone. The taut *pars tensa* is connected to the sulcus by means of the tympanic annulus (*annulus fibrosus tympanicus*), the thickened rim of the membrane [138]. The smaller, thicker but more flexible *pars flaccida* fills the notch of Rivinus superiorly.

The tympanic membrane appears as a semi-transparent, oval structure when examined from the external ear canal. From the lateral aspect, the division between *pars tensa* and *pars flaccida* is demarcated by the lateral process of the malleus, which forms a bulge in the membrane known as the malleolar prominence. The manubrium of the malleus extends from here to the centre of the *pars tensa*, attaching to its medial side. From the medial aspect, the division between the *pars tensa* and the *pars flaccida* is demarcated by the ligamentous anterior and posterior malleolar folds, which

hold the lateral process of the malleus in place. Within these folds lies the chorda tympani nerve, as it passes medial to the tympanic membrane.

The *pars tensa* takes the shape of a shallow cone, and the apex of this cone as seen from the ear canal is known as the umbo. Although the umbo is indented into the middle ear cavity, the membrane surrounding this bulges outwards, except where it is connected to the manubrium. The outer circumference of the tympanic membrane is oriented at an angle to the external auditory meatus, such that the surface area of the *pars tensa* is increased relative to the perpendicular meatus cross section [139].

Incoming sound waves cause vibration of the *pars tensa*, with the energy being transmitted to the inner ear by the coupling of the membrane to the ossicular chain via the manubrium. Vibratory amplitude can be modulated by contraction of the tensor tympani, which pulls the manubrium medially, increasing the tension of the *pars tensa* [140]. The *pars flaccida* is believed to play only a minor acoustic role in humans [141].

The Eustachian Tube

The Eustachian tube (Fig. 4.8a) comprises three anatomical parts: a bony lateral third, a fibrocartilaginous anteromedial portion and a junctional region where the bone and cartilage overlap over 3–4 mm [144]. Surrounded by soft tissue and muscles, it connects the tympanic orifice in the anterior wall of the middle ear to the nasopharyngeal orifice, which is posterior to the inferior nasal concha and lateral to the adenoid pad. The Eustachian tube is predominantly lined by a cili-

ated, pseudostratified, columnar epithelium, with non-ciliated and goblet cells being more crowded at the bone–cartilage junction [17, 145]. The cilia assist in secretion clearance by sweeping the mucus and debris towards the nasopharynx.

In a study of 286 non-cadaveric Eustachian tubes imaged with cone beam computed tomography (143 subjects), the shortest measured adult tube was 34.5 mm and the longest 47.2 mm [146]. The average length was 40.3 mm. The bony portion was approximately 1 mm longer in males than in females, and the cartilaginous portion was 1.5 mm longer [146]. The narrow ET descends anteromedially, with the cartilaginous part at an angle of approximately 35° in adults [146]. The slope of the fibrocartilaginous portion of the Eustachian tube relative to the horizontal plane was approximately 2° shallower on the right side, with a corresponding increase of 0.5 mm in the length of the right bony portion, explained by the lower *fossa cranii media* on the right [146].

The 12-mm-long bony portion [146] passes through the petrous temporal bone where it is crossed by the horizontal segment of the internal carotid artery passing medially in its carotid canal [147]. Bone rigidity prevents tubal occlusion by external pressure along this portion. The fibrocartilaginous portion is comprised of a flanged plate of cartilage posteromedially, with fibrous tissue making up the anterolateral wall [148].

The pharyngeal and tympanic ends of the ET are both wider than the central section. In the nasopharynx, the ostium is visible as the tubal elevation known as the *torus tubarius*, where the mucosa is lifted by the end of the cartilage [146]. Posterior to this lies the fossa of Rosenmüller, a common site for nasopharyngeal carcinoma. The narrowest

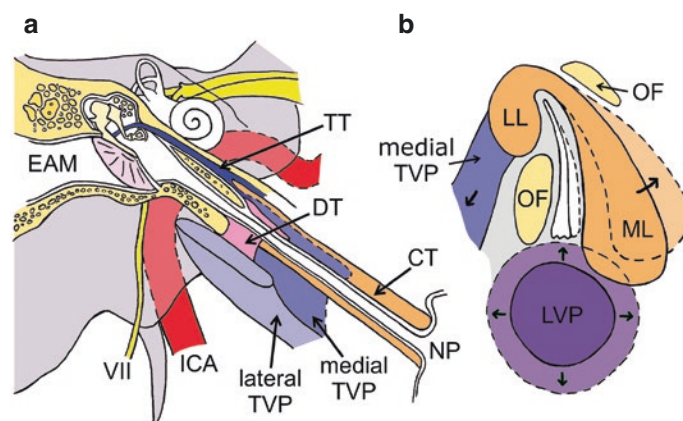


Fig. 4.8 (a) Schematic cross section of the Eustachian tube. Dilator tubae adjoins the membranous Eustachian tube at the isthmus. The medial tensor veli palatini attaches to the lateral lamina of the cartilaginous Eustachian tube. The levator veli palatini is not pictured. (b) Dilatation of the Eustachian tube lumen (central white space) by the contraction of associated muscles, based in part on the studies by Ishijima et al. [142] and Smith et al. [143]. The tensor veli palatini acts

on the superior and medial portions of the Eustachian tube, whereas the levator veli palatini predominantly acts on the inferior portion. CT, cartilaginous portion of the Eustachian tube; DT, dilatator tubae; EAM, external auditory meatus; ICA, internal carotid artery; LL, lateral lamina of the tubal cartilage; LVP, levator veli palatini; ML, medial lamina of the tubal cartilage; OF, Ostmann fat pads (medial and lateral); TVP, tensor veli palatini

part of the Eustachian tube lumen, known as the isthmus, usually lies within the cartilaginous part of the tube, near the junctional region [50, 144]. In a study of nine temporal bones, the narrowest part of the tube measured $0.65 \text{ mm}^2 \pm 0.22 \text{ mm}^2$ in cross-sectional area and lay $3.1 \text{ mm} \pm 1.6 \text{ mm}$ from the pharyngeal margin of the junctional region [144].

Functions of the Eustachian Tube

The Eustachian tube has three main functions in adults: (1) periodic ventilation of the middle ear cavity to equalise pressure with ambient atmospheric pressure, a requirement for appropriate impedance matching across the middle ear, (2) unidirectional mucociliary drainage of middle ear secretions and (3) protection of the middle ear from ascending nasopharyngeal microorganisms and sound.

At rest, the fibrocartilaginous part of the tube in the parapharyngeal space is passively closed by elastic recoil of the elastin hinge found between the lateral and medial cartilaginous laminae [149] and pressure from the adjacent Ostmann fat pads [150]. It opens actively for brief periods (around 200 ms: [151]) on swallowing and yawning and passively with high nasopharyngeal pressures such as those achieved by the Valsalva manoeuvre. Three muscles are generally believed to be involved in active Eustachian tube functions: the tensor veli palatini, levator veli palatini and salpingopharyngeus. Their innervation was considered in the earlier section on their development.

The medial bundle of the tensor veli palatini typically arises from the middle to superior lateral lamina of the fibrocartilaginous portion of the Eustachian tube [142]. Where it attaches to and dilates the isthmus it is known as the dilatator tubae muscle [152]. It joins the lateral bundle of the tensor veli palatini to wrap around the hamulus of the medial pterygoid, before inserting into the palatal aponeurosis and posterior edge of the hard palate [142]. Tensor veli palatini contraction is believed to open the middle and superior cartilaginous portions of the Eustachian tube, including the isthmus [142]. A diagrammatic illustration of how the tube is opened is presented in Fig. 4.8b.

The most inferior cartilaginous portion of the Eustachian tube is believed to be opened primarily by the contraction of the levator veli palatini muscle [142]. Arising from the inferior aspect of the petrous temporal bone, the levator veli palatini descends to pass between the tensor veli palatini and salpingopharyngeus to attach to the superior surface of the soft palate aponeurosis. This muscle does not attach to the Eustachian tube but forms a sling, passing in close proximity to the medial cartilaginous lamina [142]. By increasing its cross-sectional area, levator veli palatini contraction is believed to displace the medial lamina, elevating and rotating it to open the inferior lumen of the cartilaginous Eustachian tube [142].

The salpingopharyngeus muscle originates from the cartilaginous portion of the Eustachian tube and courses inferiorly to form the salpingopharyngeal fold, eventually attaching to the lateral pharyngeal wall. The size and presence of this muscle has been reported to be variable across individuals [153], leading to the suggestion that it lacks any significant role in Eustachian tube function. However, salpingopharyngeus dysfunction has been implicated in myogenic tinnitus associated with palatal tremor [154].

Two additional muscles have been implicated in normal Eustachian tube function: the medial and lateral pterygoid muscles. Innervated by V_3 [155], contraction of these muscles appears to enhance Eustachian tube dilatation achieved by the tensor veli palatini and levator veli palatini, but it is not necessary or sufficient to achieve Eustachian tube opening [156]. In fact, the exact mechanism by which muscular contraction results in middle ear aeration remains disputed.

The Ossicular Chain

As in all mammals, the human ossicular chain consists of three tiny bones suspended within the tympanic cavity. These bones conduct sound from the tympanic membrane to the fluid-filled inner ear, via the oval window. Although largely made of compact bone, there are vascular channels and cavities within the ossicles, which are in communication with the external supplying vessels, as described and illustrated by Manoharan et al. [157].

The adult human malleus (Figs. 4.7 and 4.9a) measures approximately 8 mm along its longest axis, from the manubrial tip to the top of the head, and typically weighs around 25 mg [158]. The malleus is likened to a hammer because of its long, tapering manubrium ('handle'), above which is a rounded head. The head has a posterior articulation facet for the incus, described later; between the head and the manubrium is a more constricted region called the neck. The lateral edge of the manubrium is attached to the *pars tensa* of the tympanic membrane; dorsally, it projects out from the neck of the malleus to form the lateral process ('*processus brevis*'), which is attached to the dorsal margin of the *pars tensa*. The connection between the manubrium and membrane is tightest at the umbo and lateral process, although there is substantial inter-individual variability in the size of this connection that must be accounted for in finite element models [159]. The thin anterior process of the malleus extends from the neck region to form an articulation with the anterior wall of the tympanic cavity, by means of the anterior malleal ligament [97]. The smaller lateral and superior ligaments attach to the lateral process and malleus head, respectively, whereas the tensor tympani tendon inserts on the manubrial base, medially [160, 161]. The positions of these attachments vary significantly between individuals.

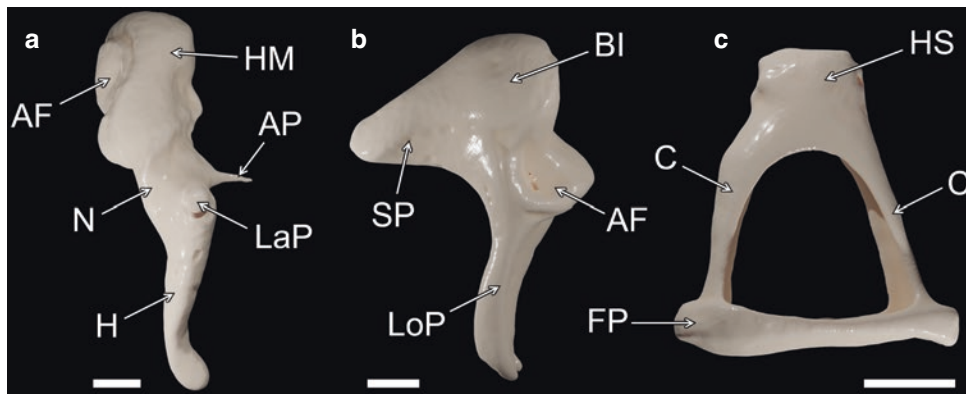


Fig. 4.9 Micro-CT reconstructions of the human ossicular chain. (a) Right malleus, lateral view; (b) right incus, lateral view; (c) right stapes, ventral view. Scale bars = 1 mm. *AF*, articulation facet (of the malleus or incus); *AP*, anterior process; *BI*, body of the incus (*corpus incudis*); *C*, stapedial crus (anterior and posterior); *FP*, footplate (*basis stapedis*);

H, handle (*manubrium mallei*); *HM*, head of the malleus (*caput mallei*); *HS*, head of the stapes (*caput stapedis*); *LaP*, lateral process; *LoP*, long process (*crus longum*); *N*, neck (*collum mallei*); *SP*, short process (*crus brevis*)

The second bone of the ossicular chain, the incus (Figs. 4.7 and 4.9b), measures roughly 6.5 mm along the axis of the long process and has a mass of around 27–28 mg [158]. The bulky body of the incus has an anterior articulation facet for the malleus and two processes extending from it. The long process is narrow, extending ventrally and bending medially at its tip, where it tapers into a narrow pedicle that supports the lenticular apophysis for articulation with the stapes. The tiny, disc-shaped lenticular apophysis was once believed to represent a fourth ossicle [162], but a thin pedicle connecting it to the incus was confirmed in 97% of 270 human specimens [163]. The blood supply to this region comes from intraosseous vessels running down the incudal long process as well as from mucosal vessels [164]. Erosion of the long process can disrupt the internal vessels, potentially making the distal part of the process more vulnerable to surgical insults [157]. The short process of the incus is stout and conical, extending posteriorly from the body. The main ligamentous attachment of the incus is its posterior ligament, which connects the end of the short process to the *fossa incudis* in the posterior tympanic cavity. This ligament extends both laterally and medially to the short process and is thicker laterally [161]. A thin superior ligament of the incus is also described [160]. Additional support is provided by the incudomalleolar articulation as well as the articulation between the lenticular apophysis and the head of the stapes.

The smallest bone of the ossicular chain is the stapes (Figs. 4.7 and 4.9c). The head is little more than a flattened, oval articulation facet for the lenticular apophysis of the incus. It is attached to a neck region, which, on its posterior aspect, provides the insertion point for the stapedius muscle. The neck diverges medially to form the two crura, which attach to either end of the footplate. The crura and neck are internally hollowed by a sulcus, which opens into the inter-

crural foramen. The stapes footplate itself fits snugly within the oval window (Fig. 4.7); its thickened rim is anchored to the rim of the oval window by means of an annular ligament. Although usually regarded as a fibrous connection, small joint cavities were found in 70% of human stapediovestibular joints [165]. The perpendicular distance from the footplate to the most distant point of the stapes head is approximately 3.3 mm, whereas the length of the long axis of the footplate averages around 2.8 mm [166]. The mass of the entire ossicle is approximately 3 mg [158]. The stapes provides input to the cochlea through motion of the footplate within the oval window.

Two joints separate the bones of the ossicular chain. The malleus head and incus body within the epitympanum have been likened in shape to ‘two lovers kissing in a small closet’ [167]. More prosaically, the malleoincudal articulation is a diarthrodial joint with saddle-shaped articular surfaces covered by a layer of hyaline cartilage [168]. Another diarthrodial joint, the incudostapedial articulation, connects the lenticular apophysis of the incus and the head of the stapes. A narrow space lined by synovium is located between these two cartilaginous joint surfaces, which are enveloped by a substantial joint capsule [163]. Whilst modelling suggests that these flexible joints will reduce the transmission of sound energy through the ossicular chain, they may protect the inner ear from high-amplitude static pressure changes [169].

Middle Ear Muscles

The tensor tympani muscle, around 25 mm long, attaches medially to the greater wing of the sphenoid, passes around the cochleariform process and inserts on the medial side of

the malleus, where the manubrium meets the neck. Recent work has confirmed the anatomical connection by means of a common tendon between the tensor tympani and tensor veli palatini muscles in adult humans [170, 171], reflecting the embryonic connection mentioned earlier. The functional significance of this connection remains unclear, as indeed is the function of the tensor tympani itself [172, 173].

The 6-mm-long stapedius muscle inserts on the neck of the stapes after arising from the pyramidal eminence of the posterosuperior mesotympanum (Fig. 4.7). Reflex contraction in response to intense acoustic stimulation results in stiffening of the annular ligament, which connects the stapes footplate to the rim of the oval window, which should serve to reduce low-frequency sound transmission [174]. Evidence suggests that this protects the inner ear from noise damage, minimises the masking of speech frequencies by loud background noise and reduces self-stimulation from vocalisation [175].

The Nerves of the Middle Ear

Four cranial nerves provide innervation to the structures of the middle ear. These are the trigeminal nerve (V), facial nerve (VII), glossopharyngeal nerve (IX) and vagus nerve (X).

The lateral surface of the tympanic membrane receives sensory innervation from the auriculotemporal branch of the trigeminal nerve, the glossopharyngeal nerve and the auricular branches of the facial and vagus nerves. The medial surface of the tympanic membrane is innervated by the tympanic nerve (a branch of the glossopharyngeal nerve also named Jacobson's nerve), which also provides general sensory innervation to the tympanic cavity via the tympanic plexus. Motor function is provided by the medial pterygoid branch of the trigeminal nerve to the tensor tympani and the stapedial branch of the facial nerve to the stapedius muscle. Sympathetic innervation is provided by the caroticotympanic nerve, which arises from the internal carotid sympathetic plexus to join the tympanic plexus.

The motor root of the facial nerve and *nervus intermedius* (containing sensory and parasympathetic fibres) pass through the internal auditory meatus to enter the Z-shaped facial (Fallopian) canal, wherein they fuse to form the facial nerve. The facial canal passes between the cochlea and vestibule, turning posteriorly at the geniculate ganglion. Within this part of the facial canal, the labyrinthine segment of the facial nerve gives off three branches: the greater superficial petrosal nerve (carrying parasympathetic innervation to the lacrimal gland and taste sensation from the palate), the lesser petrosal nerve and the external petrosal nerve. The facial nerve then traverses the medial wall of the middle ear cavity

within the facial canal, directly inferior to the lateral semicircular canal, as the tympanic segment. In the facial canal between the pyramidal eminence and stylomastoid foramen, the facial nerve is termed the 'mastoid segment', giving off three further branches:

- The motor nerve to the stapedius muscle
- The chorda tympani, which provides taste sensation to the anterior two-thirds of the tongue and parasympathetic innervation to the submandibular and sublingual salivary glands [176]
- A sensory branch that joins the auricular branch of the vagus nerve, conveying sensation from the pinna and ear canal

The facial nerve leaves the facial canal at the stylomastoid foramen, providing motor function to the *m. digastricus*, *m. stylohyoideus* and muscles of facial expression [177]. Dehiscence of the canal of the facial nerve can occur, resulting in an exposed facial nerve.

When originating from the lateral side of the facial nerve, the chorda tympani ascends and courses anteriorly into the middle ear [178]. However, when originating from the posterolateral side, the chorda tympani forms a posteriorly convex curve on ascending, before passing anteriorly into the middle ear, thus bulging into the anterior portion of the mastoid complex [178]. Occasionally, the chorda tympani originates inferior to the stylomastoid foramen, outside the facial canal [178]. The chorda tympani enters the tympanic cavity via the posterior canaliculus, on a level with the handle of the malleus and round window. It arches upwards and forwards to cross the *pars flaccida*, passing medially to the neck of the malleus and just dorsally to the insertion of the tensor tympani tendon, before exiting the tympanic cavity through the anterior canaliculus [176].

As the first branch arising from the petrous ganglion of the glossopharyngeal nerve, the tympanic nerve ascends through the tympanic canaliculus to emerge onto the cochlear promontory, where it branches and coalesces with branches of the caroticotympanic nerve to form the tympanic plexus. The plexus is variably located in submucosal open grooves and bony canals over the promontory, supplying sensation and autonomic innervation [179] to the tympanic cavity and medial surface of the tympanic membrane. Tympanic plexus somatic fibres are postulated to provide the afferent pathway by which middle ear aeration could be regulated [180]. However, evidence in humans is inconclusive [181]. The tympanic nerve exits the middle ear through or near the canal for the tensor tympani muscle as the lesser superficial petrosal nerve [182], conveying presynaptic parasympathetic fibres to the otic ganglion. Post-ganglionic fibres travel with the auriculotemporal nerve (a branch of V_3) to provide para-

sympathetic secretomotor innervation to the parotid gland. Tympanic neurectomy has been used in the management of Frey's syndrome [183].

The Mastoid Complex

Lying within the mastoid process of the temporal bone, the mastoid complex (Figs. 4.1 and 4.6) is a collection of interconnected, air-filled spaces lined by a thin, flat epithelium with a dense underlying capillary network [184]. These air-filled spaces are in communication with the epitympanum via the *aditus ad antrum*. This connection allows unrestricted movement of gas between the mastoid complex and middle ear cavity.

As mentioned earlier, the extent of pneumatisation of the mastoid can vary greatly between individuals, from well-pneumatised to acellular or sclerotic. The well-pneumatised adult mastoid cavity can be subdivided into two areas: the mastoid antrum (and central tract) and the peripheral area [119]. Lying at the same level as the spine of Henle in the external ear canal, the mastoid antrum is a cave-like space that extends inferiorly and laterally to form the oblong central tract. It is surrounded by smaller, thin-walled cavities known as the peripheral air cells that can be subdivided by location but are variable in size, number and distribution [119]. As a result, the total gaseous volume of the pneumatised mastoid complex can vary greatly. A recent high-resolution micro-computed tomography (micro-CT) study has produced volumes of 2.7–13.6 cm³, with a corresponding mucosal surface area of 81–326 cm² [185].

The tegmen tympani forms the roof of the mastoid complex, separating the mastoid air cells from the middle cranial fossa [186]. On the surface, this margin is approximated by the temporal line at the inferior limit of the temporal muscle [186]. The anterior boundary of the mastoid complex comprises the *aditus ad antrum* superiorly and the bony canal for the descending facial nerve inferiorly. A thin plate of bone separates the mastoid antrum from the descending sigmoid sinus, marking the posterior limit of the mastoid complex. However, pneumatisation can occur throughout the temporal bone. Thereby, peripheral air cells can be present outside the boundaries of the mastoid complex.

On the medial wall of the mastoid complex, the bony prominence demarcating the lateral semicircular canal can be located near the *aditus ad antrum*. The posterior semicircular canal lies deep to the remainder of the medial wall of the mastoid complex. The medial wall itself is defined as the thin plates of bone overlying these semicircular canals. The lateral wall is a thick, bony layer identifiable as the squamous part of the temporal bone inferior to the supramastoid

crest. Towards the occiput, up to four mastoid emissary veins may perforate the superficial petromastoid surface, on average 35 mm along a line drawn from the mastoid tip to the asterion [187]. In some subjects, these vessels may be absent [187].

Within the mastoid, a bony plate dividing the superficial squamous air cells from the petrous air cells and mastoid antrum may be present in some individuals. Known as Körner's septum, this structure results from the incomplete fusion and obliteration of the fetal petrosquamosal suture. This is believed to contribute to attic blockage and has been correlated with the presence of chronic otitis media and its complications [188]. It has surgical relevance during mastoidectomy, as failure to remove Körner's septum results in failure to locate the mastoid antrum. MacEwen's (suprameatal) triangle [189] is used to locate the mastoid antrum from surface anatomy.

The mastoid cavities are widely believed to contribute to middle ear pressure regulation via membrane gas exchange [190, 191] and passive 'air buffering' [192]. Gas exchange and aeration of the mastoid complex are dependent on an intact mastoid mucosa [193]. The mucosa has two characteristics supporting this function: (1) a short diffusion distance provided by the flattened epithelial cells and proximity to the underlying capillaries and (2) a high surface area generated by cellular pneumatisation. Through its communication with the middle ear cavity, gas exchange across the mastoid mucosa can produce gradual pressure changes within the middle ear cavity [191]. This pressure regulation activity may complement that of the Eustachian tube, which acts to produce larger and more rapid changes in pressure [191], and the mastoid cavities have been postulated to slow down the decline of middle ear pressure during periods of Eustachian tube dysfunction [190]. However, a mastoid cavity is not required to achieve normal middle ear pressure in the context of a functioning Eustachian tube [194], and some mathematical modelling has opposed the postulated function of the mastoid complex as a gas reserve [195].

Alternative or additional functions of the mastoid cavities, which have been proposed, include frequency-dependent impedance modulation affected by the anatomical layout of air cell networks [196], middle and inner ear temperature regulation [197], protection of intracranial structures from lateral trauma [198] and reduction of skull density [199]. However, the variability in development of the mastoid cavities among individuals shows that a well-defined morphology and volume of the mastoid complex is not vital to function; indeed, cellular mastoid cavities are lacking in most non-primates, including all common laboratory mammals. Some authors have suggested that the mastoid complex in humans has no adaptive function [200].

Conclusions

Our current knowledge of middle ear development comes from nearly two centuries of research, with much of it based on the detailed comparison of wax-embedded, serial sections. What we know about postnatal middle ear anatomy in humans comes largely from surgical observations and temporal bone dissections, again dating back centuries. However, the advent of molecular biology techniques has led, over the last 30 years, to a revolution in our understanding of the mechanisms of middle ear development while the increased availability and resolution of micro-computed tomography allows us to explore the anatomy in even more detail. This work is not yet finished. Questions remain regarding how appropriate mice are as models for human middle ear development, given the many differences in ear structure between the two species. Although adult human middle ear morphology is extremely well-described, the functions of some of its prominent features, including the tensor tympani, mastoid complex and *pars flaccida* of the tympanic membrane, are still very poorly understood. More detailed studies of how anatomical variations correlate with middle ear pathologies may help address this. After a long period of relative stasis, our knowledge of the human middle ear is now increasing exponentially; we very much expect that there will be many changes to be made in the future editions of this book!

Acknowledgements Temporal bone specimens from which CT reconstructions were made were obtained from the Human Anatomy Centre, Department of Physiology, Development & Neuroscience, University of Cambridge. Prior to decease, all donors had provided consent for the use of their bodies for anatomical research, in compliance with the Human Tissue Act 2004. The authors thank Will Ashley-Fenn, Darren Broadhurst, Sue Jones, Prabhvir Marway and Maria Wright for preparation of the temporal bone specimens that we used and Cecilia Brassett and Richard Lloyd for their help with project logistics and permissions. CT scans were conducted at the Cambridge Biotomography Centre.

References

1. Grevellec A, Tucker AS. The pharyngeal pouches and clefts: development, evolution, structure and derivatives. *Semin Cell Dev Biol.* 2010;21:325–32.
2. Mallo M. Formation of the middle ear: recent progress on the developmental and molecular mechanisms. *Dev Biol.* 2001;231:410–9.
3. Graham A, Poopalasundaram S, Shone V, Kiecker C. A reappraisal and revision of the numbering of the pharyngeal arches. *J Anat.* 2019;235:1019–23.
4. Sudler MT. The development of the nose, and of the pharynx and its derivatives in man. *Am J Anat.* 1902;1:391–416.
5. Benson MT, Dalen K, Mancuso AA, Kerr HH, Cacciarelli AA, Mafee MF. Congenital anomalies of the branchial apparatus: embryology and pathologic anatomy. *Radiographics.* 1992;12:943–60.
6. Quinlan R, Martin P, Graham A. The role of actin cables in directing the morphogenesis of the pharyngeal pouches. *Development.* 2004;131:593–9.
7. van Waegeningh HF, Ebbens FA, van Spronsen E, Oostra R-J. Single origin of the epithelium of the human middle ear. *Mech Dev.* 2019;158:103556.
8. Burford CM, Mason MJ. Early development of the malleus and incus in humans. *J Anat.* 2016;229:857–70.
9. Frazer JE. The second visceral arch and groove in the tubotympanic region. *J Anat Physiol.* 1914;48:391–408.
10. Kanagasuntheram R. A note on the development of the tubotympanic recess in the human embryo. *J Anat.* 1967;101:731–41.
11. Anson BJ, Bast TH, Cauldwell EW. The development of the auditory ossicles, the otic capsule and the extracapsular tissues. *Ann Otol Rhinol Laryngol.* 1948;57:603–32.
12. Guggenheim P, Clements L, Schlesinger A. The significance and fate of the mesenchyme of the middle ear. *Laryngoscope.* 1956;66:1303–26.
13. Tucker AS. Major evolutionary transitions and innovations: the tympanic middle ear. *Philos Trans Royal Soc B Biol Sci.* 2017;372:20150483.
14. Wittmaack K. Über die normale end die pathologische Pneumatisation des Schläfenbeines einschliesslich ihrer Beziehungen zu den Mittelohrerkrankungen. Jena: Verlag von Gustav Fischer; 1918.
15. Schwarzbart A. The pneumatization of the temporal bone: a new concept. *J Laryngol Otol.* 1959;73:45–7.
16. Thompson H, Tucker AS. Dual origin of the epithelium of the mammalian middle ear. *Science.* 2013;339:1453–6.
17. Akaan-Penttilä E. Middle ear mucosa in newborn infants. A topographical and microanatomical study. *Acta Otolaryngol.* 1982;93:251–9.
18. Lim DJ. Normal and pathological mucosa of the middle ear and eustachian tube. *Clin Otolaryngol Allied Sci.* 1979;4:213–32.
19. Sade J. Middle ear mucosa. *Arch Otolaryngol.* 1966;84:137–43.
20. Piza J, Northrop C, Eavey RD. Embryonic middle ear mesenchyme disappears by redistribution. *Laryngoscope.* 1998;108:1378–81.
21. Piza JE, Northrop CC, Eavey RD. Neonatal mesenchyme temporal bone study: typical receding pattern versus increase in Potter's sequence. *Laryngoscope.* 1996;106:856–64.
22. Nikolic P, Järleback LE, Billett TE, Thorne PR. Apoptosis in the developing rat cochlea and its related structures. *Brain Res Dev Brain Res.* 2000;119:75–83.
23. Roberts DS, Miller SA. Apoptosis in cavitation of middle ear space. *Anat Rec.* 1998;251:286–9.
24. Palva T, Ramsay H. Fate of the mesenchyme in the process of pneumatization. *Otol Neurotol.* 2002;23:192–9.
25. Presley R. Lizards, mammals and the primitive tetrapod tympanic membrane. *Symp Zool Soc Lond.* 1984;52:127–52.
26. Minoux M, Kratochwil CF, Ducret S, Amin S, Kitazawa T, Kurihara H, Bobola N, Vilain N, Rijli FM. Mouse *Hoxa2* mutations provide a model for microtia and auricle duplication. *Development.* 2013;140:4386–97.
27. Ars B. Organogenesis of the middle ear structures. *J Laryngol Otol.* 1989;103:16–21.
28. Michaels L. Evolution of the epidermoid formation and its role in the development of the middle ear and tympanic membrane during the first trimester. *J Otolaryngol.* 1988a;17:22–8.
29. Michaels L. Origin of congenital cholesteatoma from a normally occurring epidermoid rest in the developing middle ear. *Int J Pediatr Otorhinolaryngol.* 1988b;15:51–65.
30. Lee TS, Liang JN, Michaels L, Wright A. The epidermoid formation and its affinity to congenital cholesteatoma. *Clin Otolaryngol Allied Sci.* 1998;23:449–54.

31. Mallo M, Gridley T. Development of the mammalian ear: coordinate regulation of formation of the tympanic ring and the external acoustic meatus. *Development*. 1996;122:173–9.
32. Rivera-Pérez JA, Mallo M, Gendron-Maguire M, Gridley T, Behringer RR. *Gooseoid* is not an essential component of the mouse gastrula organizer but is required for craniofacial and rib development. *Development*. 1995;121:3005–12.
33. Yamada G, Mansouri A, Torres M, Stuart ET, Blum M, Schultz M, De Robertis EM, Gruss P. Targeted mutation of the murine *gooseoid* gene results in craniofacial defects and neonatal death. *Development*. 1995;121:2917–22.
34. Yamada G, Ueno K, Nakamura S, Hanamura Y, Yasui K, Uemura M, Eizuru Y, Mansouri A, Blum M, Sugimura K. Nasal and pharyngeal abnormalities caused by the mouse *gooseoid* gene mutation. *Biochem Biophys Res Commun*. 1997;233:161–5.
35. Parry DA, Logan CV, Stegmann AP, Abdelhamed ZA, Calder A, Khan S, Bonthron DT, Clowes V, Sheridan E, Ghali N, Chudley AE, Dobbie A, Stumpel CT, Johnson CA. SAMS, a syndrome of short stature, auditory-canal atresia, mandibular hypoplasia, and skeletal abnormalities is a unique neurocristopathy caused by mutations in *Gooseoid*. *Am J Hum Genet*. 2013;93:1135–42.
36. Mallo M, Schrewe H, Martin JF, Olson EN, Ohnemus S. Assembling a functional tympanic membrane: signals from the external acoustic meatus coordinate development of the malleal manubrium. *Development*. 2000;127:4127–36.
37. Ishimoto S, Ito K, Kondo K, Yamasoba T, Kaga K. The role of the external auditory canal in the development of the malleal manubrium in humans. *Arch Otolaryngol Head Neck Surg*. 2004;130:913–6.
38. Mayer TE, Brueckmann H, Siebert R, Witt A, Weerda H. High-resolution CT of the temporal bone in dysplasia of the auricle and external auditory canal. *AJNR Am J Neuroradiol*. 1997;18:53–65.
39. Adanır SS, Bahşi İ. The giant anatomist, whose value is later understood: Bartolomeo Eustachi. *Childs Nerv Syst*. 2021;37:1–4.
40. Tos M. Growth of the foetal Eustachian tube and its dimensions. *Archiv Fur Klinische Und Experimentelle Ohren- Nasen- Und Kehlkopfheilkunde*. 1971;198:177–86.
41. Church MW, Gerkin KP. Hearing disorders in children with fetal alcohol syndrome: findings from case reports. *Pediatrics*. 1988;82:147–54.
42. Magnuson B, Falk B. Diagnosis and management of eustachian tube malfunction. *Otolaryngol Clin N Am*. 1984;17:659–71.
43. Todd NW. Otitis media and eustachian tube caliber. *Acta Otolaryngol Suppl*. 1983;404:1–17.
44. Swarts JD, Rood SR, Doyle WJ. Fetal development of the auditory tube and paratubal musculature. *Cleft Palate J*. 1986;23:289–311.
45. Anthwal N, Thompson H. The development of the mammalian outer and middle ear. *J Anat*. 2016;228:217–32.
46. Tono T, Schachern PA, Morizono T, Paparella MM, Morimitsu T. Developmental anatomy of the supratubal recess in temporal bones from fetuses and children. *Am J Otol*. 1996;17:99–107.
47. Tamari MJ. Auditory tube and tympanic cavity during embryonal, fetal, and prenatal life; histologic study. *AMA Arch Otolaryngol*. 1953;57:627–47.
48. Kitajiri M, Sando I, Takahara T. Postnatal development of the eustachian tube and its surrounding structures. Preliminary study. *Ann Otol Rhinol Laryngol*. 1987;96:191–8.
49. Luntz M, Sadé J. Growth of the eustachian tube lumen with age. *Am J Otolaryngol*. 1988;9:195–8.
50. Suzuki C, Balaban C, Sando I, Sudo M, Ganbo T, Kitagawa M. Postnatal development of Eustachian tube: a computer-aided 3-D reconstruction and measurement study. *Acta Otolaryngol*. 1998;118:837–43.
51. Ishijima K, Sando I, Balaban C, Suzuki C, Takasaki K. Length of the eustachian tube and its postnatal development: computer-aided three-dimensional reconstruction and measurement study. *Ann Otol Rhinol Laryngol*. 2000;109:542–8.
52. Oberascher G, Grobovschek M. The eustachian tube in HR computerized tomography. Imaging in the fetus, newborn infant and infant. *HNO*. 1987;35:455–61.
53. Takasaki K, Takahashi H, Miyamoto I, Yoshida H, Yamamoto-Fukuda T, Enatsu K, Kumagami H. Measurement of angle and length of the eustachian tube on computed tomography using the multiplanar reconstruction technique. *Laryngoscope*. 2007;117:1251–4.
54. Dinç AE, Damar M, Uğur MB, Öz II, Eliçora S, Bişkin S, Tutar H. Do the angle and length of the eustachian tube influence the development of chronic otitis media? *Laryngoscope*. 2015;125:2187–92.
55. De la Cuadra Blanco C, Peces Peña MD, Rodríguez-Vázquez JF, Mérida-Velasco JA, Mérida-Velasco JR. Development of the human tensor veli palatini: specimens measuring 13.6–137 mm greatest length; weeks 6–16 of development. *Cells Tissues Organs*. 2012;195:392–9.
56. Rodríguez-Vázquez JF, Sakiyama K, Abe H, Amano O, Murakami G. Fetal tendinous connection between the tensor tympani and tensor veli palatini muscles: a single digastric muscle acting for morphogenesis of the cranial base. *Anat Record (Hoboken)*. 2016;299:474–83.
57. Kishimoto H, Yamada S, Kanahashi T, Yoneyama A, Imai H, Matsuda T, Takeda T, Kawai K, Suzuki S. Three-dimensional imaging of palatal muscles in the human embryo and fetus: development of levator veli palatini and clinical importance of the lesser palatine nerve. *Dev Dyn*. 2016;245:123–31.
58. Logjes RJ, Bleys RL, Breugem CC. The innervation of the soft palate muscles involved in cleft palate: a review of the literature. *Clin Oral Investig*. 2016;20:895–901.
59. Fuchs JC, Linden JF, Baldini A, Tucker AS. A defect in early myogenesis causes otitis media in two mouse models of 22q11.2 deletion syndrome. *Hum Mol Genet*. 2015;24:1869–82.
60. Diogo R, Abdala V, Lonergan N, Wood BA. From fish to modern humans—comparative anatomy, homologies and evolution of the head and neck musculature. *J Anat*. 2008;213:391–424.
61. McMyn JK. The anatomy of the salpingo-pharyngeus muscle. *J Laryngol Otol*. 1940;55:1–22.
62. Warmbrunn MV, de Bakker BS, Hagoort J, Alefs-de Bakker PB, Oostra R-J. Hitherto unknown detailed muscle anatomy in an 8-week-old embryo. *J Anat*. 2018;233:243–54.
63. Gaupp E. Die Reichertsche Theorie (Hammer-, Amboss- und Kieferfrage). *Archiv für Anatomie und Entwicklungsgeschichte (suppl)*. 1913;1912:1–416.
64. Strickland EM, Hanson JR, Anson BJ. Branchial sources of auditory ossicles in man. I. Literature. *Arch Otolaryngol*. 1962;76:100–22.
65. Reichert C. Ueber die Visceralbogen der Wirbelthiere im Allgemeinen und deren Metamorphosen bei den Vögeln und Säugethieren. *Archiv für Anatomie, Physiologie und Wissenschaftliche Medicin*. 1837;1837:120–222.
66. Wyganowska-Świątkowska M, Przystańska A. The Meckel's cartilage in human embryonic and early fetal periods. *Anat Sci Int*. 2011;86:98–107.
67. Hanson JR, Anson BJ. Development of the malleus of the human ear. Illustrated in atlas series. *Q Bull Northwest Univ Med Sch*. 1962;36:119–37.
68. Rodríguez-Vázquez JF, Mérida-Velasco JR, Jiménez-Collado J. A study of the os goniale in man. *Cells Tissues Organs*. 1991;142:188–92.
69. Tucker AS, Watson RP, Lettice LA, Yamada G, Hill RE. *Bapx1* regulates patterning in the middle ear: altered regulatory role in the transition from the proximal jaw during vertebrate evolution. *Development*. 2004;131:1235–45.

70. Gendron-Maguire M, Mallo M, Zhang M, Gridley T. Hoxa-2 mutant mice exhibit homeotic transformation of skeletal elements derived from cranial neural crest. *Cell*. 1993;75:1317–31.
71. Rijli FM, Mark M, Lakkaraju S, Dierich A, Dollé P, Chambon P. A homeotic transformation is generated in the rostral branchial region of the head by disruption of Hoxa-2, which acts as a selector gene. *Cell*. 1993;75:1333–49.
72. Hanson JR, Anson BJ, Strickland EM. Branchial sources of the auditory ossicles in man. II. Observations of embryonic stages from 7 mm to 28 mm (CR length). *Arch Otolaryngol*. 1962;76:200–15.
73. Louryan S. Le développement des osselets de l'ouïe chez l'embryon humain: corrélations avec les données recueillies chez la souris. *Bull Assoc Anat*. 1993;77:29–32.
74. Whyte J, Cisneros A, Yus C, Fraile J, Obón J, Vera A. Tympanic ossicles and pharyngeal arches. *Anat Histol Embryol*. 2009;38:31–3.
75. Harrison MS, Leeming R. Preservation of the stapedius tendon in surgery of the stapes. *Br J Audiol*. 1971;5:78–84.
76. Standring S, Ellis H, Healy JC, Johnson D, Williams A, editors. *Gray's anatomy: the anatomical basis of clinical practice*. 39th ed. Edinburgh: Elsevier Churchill Livingstone; 2005.
77. Williams PL, Bannister LH, Berry MM, Collins P, Dyson M, Dussek JE, Ferguson MWJ, editors. *Gray's Anatomy*. 38th ed. Edinburgh: Churchill Livingstone; 1995.
78. Williams PL, Warwick R, Dyson M, Bannister LH, editors. *Gray's anatomy*. 37th ed. Edinburgh: Churchill Livingstone; 1989.
79. Rodríguez-Vázquez JF, Yamamoto M, Abe S, Katori Y, Murakami G. Development of the human incus with special reference to the detachment from the chondrocranium to be transferred into the middle ear. *Anat Record (Hoboken)*. 2018;301:1405–15.
80. O'Gorman S. Second branchial arch lineages of the middle ear of wild-type and Hoxa2 mutant mice. *Dev Dyn*. 2005;234:124–31.
81. Mason MJ. Of mice, moles and Guinea pigs: functional morphology of the middle ear in living mammals. *Hear Res*. 2013;301:4–18.
82. Louryan S, Lejong M, Choa-Duterte M, Vanmuylder N. Hox-A2 protein expression in mouse embryo middle ear ossicles. *Morphologie*. 2018;102:243–9.
83. Anson BJ, Cauldwell EW. The developmental anatomy of the human stapes. *Ann Otol Rhinol Laryngol*. 1942;51:891–904.
84. Rodríguez-Vázquez JF. Development of the stapes and associated structures in human embryos. *J Anat*. 2005;207:165–73.
85. Thompson H, Ohazama A, Sharpe PT, Tucker AS. The origin of the stapes and relationship to the otic capsule and oval window. *Dev Dyn*. 2012;241:1396–404.
86. Amin S, Tucker AS. Joint formation in the middle ear: lessons from the mouse and guinea pig. *Dev Dyn*. 2006;235:1326–33.
87. Anson BJ, Bast TH. The development of the auditory ossicles and associated structures in man. *Ann Otol Rhinol Laryngol*. 1946;55:467–94.
88. Whyte JR, González L, Cisneros AI, Yus C, Torres A, Sarrat R. Fetal development of the human tympanic ossicular chain articulations. *Cells Tissues Organs*. 2002;171:241–9.
89. Jahrsdoerfer RA, Aguilar EA, Yeakley JW, Cole RR. Treacher Collins syndrome: an otologic challenge. *Ann Otol Rhinol Laryngol*. 1989;98:807–12.
90. Phelps PD, Poswillo D, Lloyd GA. The ear deformities in mandibulofacial dysostosis (Treacher Collins syndrome). *Clin Otolaryngol Allied Sci*. 1981;6:15–28.
91. Rodríguez-Vázquez JF, Yamamoto M, Kim JH, Jin Z-W, Katori Y, Murakami G. The incudopetrotal joint of the human middle ear: a transient morphology in fetuses. *J Anat*. 2020;237:176–87.
92. Anson BJ, Bast TH. Development of the incus of the human ear; illustrated in atlas series. *Q Bull Northwest Univ Med Sch*. 1959;33:110–9.
93. Yokoyama T, Iino Y, Kakizaki K, Murakami Y. Human temporal bone study on the postnatal ossification process of auditory ossicles. *Laryngoscope*. 1999;109:927–30.
94. Oesterle F. Über den Feinbau der Gehörknöchelchen und seine Entstehung. *Arch Ohren Nasen Kehlkopfheilkd*. 1933;135:311–27.
95. Anson BJ, Winch TR. Vascular channels in the auditory ossicles in man. *Ann Otol Rhinol Laryngol*. 1974;83:142–58.
96. Michaelides E, Kansal A, Rutter S, Schutt C. The malleus cap: anatomic description of cartilage of the lateral process of the malleus. *Am J Otolaryngol*. 2018;39:208–11.
97. Proops D, Hawke M, Berger G, MacKay A. The anterior process of the malleus. *J Otolaryngol*. 1984;13:39–43.
98. Hitier M, Zhang M, Labrousse M, Barbier C, Patron V, Moreau S. Persistent stapedia arteries in human: from phylogeny to surgical consequences. *Surg Radiol Anat*. 2013;35:883–91.
99. Rodríguez-Vázquez JF, Mérida-Velasco JR, Verdugo-López S. Development of the stapedius muscle and unilateral agenesis of the tendon of the stapedius muscle in a human fetus. *Anat Record (Hoboken)*. 2010;293:25–31.
100. Rodríguez-Vázquez JF. Development of the stapedius muscle and pyramidal eminence in humans. *J Anat*. 2009;215:292–9.
101. Rodríguez-Vázquez JF, Mérida-Velasco JR, Verdugo-López S, Sánchez-Montesinos I, Mérida-Velasco JA. Morphogenesis of the second pharyngeal arch cartilage (Reichert's cartilage) in human embryos. *J Anat*. 2006;208:179–89.
102. Noden DM, Trainor PA. Relations and interactions between cranial mesoderm and neural crest populations. *J Anat*. 2005;207:575–601.
103. Anson BJ, Bast TH, Richany SF. The fetal development of the tympanic ring, and related structures in man. *Q Bull Northwest Univ Med Sch*. 1955;29:21–36.
104. Rodríguez-Vázquez JF, Murakami G, Verdugo-López S, Abe S-I, Fujimiya M. Closure of the middle ear with special reference to the development of the tegmen tympani of the temporal bone. *J Anat*. 2011;218:690–8.
105. Bowden RE. Development of the middle and external ear in man. *Proc R Soc Med*. 1977;70:807–15.
106. Spector GJ, Ge XX. Development of the hypotympanum in the human fetus and neonate. *Ann Otol Rhinol Laryngol Suppl*. 1981;90:1–20.
107. Eby TL. Development of the facial recess: implications for cochlear implantation. *Laryngoscope*. 1996;106:1–7.
108. Anson BJ, Bast TH. Development of the otic capsule of the human ear; illustrated in atlas series. *Q Bull Northwest Univ Med Sch*. 1958;32:157–72.
109. Sai X, Ladher RK. Early steps in inner ear development: induction and morphogenesis of the otic placode. *Front Pharmacol*. 2015;6:19.
110. Anson BJ, Bast TH. The development of the otic capsule in the region of surgical fenestration. *Q Bull Northwest Univ Med Sch*. 1949;23:465–77.
111. Nemzek WR, Brodie HA, Chong BW, Babcock CJ, Hecht ST, Salamat S, Ellis WG, Seibert JA. Imaging findings of the developing temporal bone in fetal specimens. *AJNR Am J Neuroradiol*. 1996;17:1467–77.
112. Leibovitz Z, Egenburg S, Bronshtein M, Shapiro I, Tepper R, Malinger G, Ohel G. Sonographic imaging of fetal tympanic rings. *Ultrasound Obstet Gynecol*. 2013;42:536–44.
113. Humphrey LT, Scheuer L. Age of closure of the foramen of Huschke: an osteological study. *Int J Osteoarchaeol*. 2006;16:47–60.
114. Rivera-Pérez JA, Wakamiya M, Behringer RR. Goosecoid acts cell autonomously in mesenchyme-derived tissues during craniofacial development. *Development*. 1999;126:3811–21.
115. Mason MJ. Functional morphology of rodent middle ears. In: Hautier L, Cox PG, editors. *Evolution of the rodents: advances*

- in phylogeny, functional morphology and development, vol. 5. Cambridge: Cambridge University Press; 2015. p. 373–404.
116. Bast TH, Forester HB. Origin and distribution of air cells in the temporal bone. *Arch Otolaryngol.* 1939;30:183–205.
 117. Cinamon U. The growth rate and size of the mastoid air cell system and mastoid bone: a review and reference. *Eur Arch Otorhinolaryngol.* 2009;266:781–6.
 118. Halewyck S, Louryan S, Van Der Veken P, Gordts F. Craniofacial embryology and postnatal development of relevant parts of the upper respiratory system. *B-ENT.* 2012;8(Suppl 19):5–11.
 119. Virapongse C, Sarwar M, Bhimani S, Sasaki C, Shapiro R. Computed tomography of temporal bone pneumatization: 1. Normal pattern and morphology. *AJR Am J Roentgenol.* 1985;145:473–81.
 120. Palva T, Palva A. Size of the human mastoid air cell system. *Acta Otolaryngol.* 1966;62:237–51.
 121. Crowe SJ, Polvogt LM. Embryonic tissue in the middle ear and mastoid: report of two cases. *Arch Otolaryngol.* 1930;12:151–61.
 122. Kasemsuwan L, Schachern P, Paparella MM, Le CT. Residual mesenchyme in temporal bones of children. *Laryngoscope.* 1996;106:1040–3.
 123. Jaisinghani VJ, Paparella MM, Schachern PA, Schneider DS, Le CT. Residual mesenchyme persisting into adulthood. *Am J Otolaryngol.* 1999;20:363–70.
 124. Paparella MM, Shea D, Meyerhoff WL, Goycoolea MV. Silent otitis media. *Laryngoscope.* 1980;90:1089–98.
 125. Sánchez Fernandez JM, Yarnoz J. Study of the mesenchymal clearance factor and its importance in the middle ear pneumatization process in rat and in man. *Acta Otolaryngol.* 1981;91:557–65.
 126. Bilgin H, Kasemsuwan L, Schachern PA, Paparella MM, Le CT. Temporal bone study of Down's syndrome. *Arch Otolaryngol Head Neck Surg.* 1996;122:271–5.
 127. Harada T, Sando I. Temporal bone histopathologic findings in Down's syndrome. *Arch Otolaryngol.* 1981;107:96–103.
 128. Zavadskii NV, Zavadskii AV, Ntutumu AN. Controversial issues in the treatment of recurrent purulent otitis media in young children. *Vestn Otorinolaringol.* 1990;1990:3–7.
 129. Rauchfuss A. Myxomatous remnants in the human middle ear. Histologic studies of their regression and microtopography. *Laryngol Rhinol Otol.* 1985;64:441–5.
 130. Shewel Y, Bassiouny M, Ebrahim M. Endoscopic assessment of the isthmus tympanicum and tensor tympani fold and their relationship with mastoid pneumatization in chronic otitis media. *J Int Adv Otol.* 2020;16:227–33.
 131. Dahlberg G, Diamant M. Inheritance of pneumatisation of the mastoid bone. *Hereditas.* 1945;31:441–56.
 132. Lazaridis E, Saunders JC. Can you hear me now? A genetic model of otitis media with effusion. *J Clin Investig.* 2008;118:471–4.
 133. Bluestone CD, Swarts JD. Human evolutionary history: consequences for the pathogenesis of otitis media. *Otolaryngol Head Neck Surg.* 2010;143:739–44.
 134. Depreux FF, Darrow K, Conner DA, Eavey RD, Liberman MC, Seidman CE, Seidman JG. Eya4-deficient mice are a model for heritable otitis media. *J Clin Investig.* 2008;118:651–8.
 135. Aimi K. The tympanic isthmus: its anatomy and clinical significance. *Laryngoscope.* 1978;88:1067–81.
 136. Tóth M, Alpár A, Patonay L, Oláh I. Development and surgical anatomy of the round window niche. *Ann Anat.* 2006;188:93–101.
 137. Franz BK, Clark GM, Bloom DM. Surgical anatomy of the round window with special reference to cochlear implantation. *J Laryngol Otol.* 1987;101:97–102.
 138. Kassem F, Ophir D, Bernheim J, Berger G. Morphology of the human tympanic membrane annulus. *Otolaryngol Head Neck Surg.* 2010;142:682–7.
 139. Decraemer WF, Dirckx JJ, Funnell WR. Shape and derived geometrical parameters of the adult, human tympanic membrane measured with a phase-shift moiré interferometer. *Hear Res.* 1991;51:107–21.
 140. Djupesland G. Middle ear muscle reflexes elicited by acoustic and nonacoustic stimulation. *Acta Otolaryngol Suppl.* 1964;188:287–92.
 141. Aritomo H, Goode RL, Gonzalez J. The role of pars flaccida in human middle ear sound transmission. *Otolaryngol Head Neck Surg.* 1988;98:310–4.
 142. Ishijima K, Sando I, Balaban CD, Miura M, Takasaki K. Functional anatomy of levator veli palatini muscle and tensor veli palatini muscle in association with eustachian tube cartilage. *Ann Otol Rhinol Laryngol.* 2002;111:530–6.
 143. Smith ME, Scoffings DJ, Tysome JR. Imaging of the Eustachian tube and its function: a systematic review. *Neuroradiology.* 2016;58:543–56.
 144. Sudo M, Sando I, Ikui A, Suzuki C. Narrowest (isthmus) portion of Eustachian tube: a computer-aided three-dimensional reconstruction and measurement study. *Ann Otol Rhinol Laryngol.* 1997;106:583–8.
 145. Hiraide F, Inouye T. The fine surface view of the human adult eustachian tube. *J Laryngol Otol.* 1983;97:149–57.
 146. Janzen-Senn I, Schuon RA, Tavassol F, Lenarz T, Paasche G. Dimensions and position of the Eustachian tube in humans. *PLoS One.* 2020;15:e0232655.
 147. Liu J, Pinheiro-Neto CD, Fernandez-Miranda JC, Snyderman CH, Gardner PA, Hirsch BE, Wang E. Eustachian tube and internal carotid artery in skull base surgery: an anatomical study. *Laryngoscope.* 2014;124:2655–64.
 148. Bluestone CD, Doyle WJ. Anatomy and physiology of eustachian tube and middle ear related to otitis media. *J Allergy Clin Immunol.* 1988;81:997–1003.
 149. Matsune S, Sando I, Takahashi H. Elastin at the hinge portion of the eustachian tube cartilage in specimens from normal subjects and those with cleft palate. *Ann Otol Rhinol Laryngol.* 1992;101:163–7.
 150. Aoki H, Sando I, Takahashi H. Anatomic relationships between Ostmann's fatty tissue and eustachian tube. *Ann Otol Rhinol Laryngol.* 1994;103:211–4.
 151. Alper CM, Swarts JD, Singla A, Banks J, Doyle WJ. Relationship between the electromyographic activity of the paratubal muscles and eustachian tube opening assessed by sonotubometry and videendoscopy. *Arch Otolaryngol Head Neck Surg.* 2012;138:741–6.
 152. Rood SR, Doyle WJ. Morphology of tensor veli palatini, tensor tympani, and dilator tubae muscles. *Ann Otol Rhinol Laryngol.* 1978;87:202–10.
 153. Dickson DR, Dickson WM. Velopharyngeal anatomy. *J Speech Hear Res.* 1972;15:372–81.
 154. Chien HF, Sanchez TG, Sennes LU, Barbosa ER. Endonasal approach of salpingopharyngeus muscle for the treatment of ear click related to palatal tremor. *Parkinsonism Relat Disord.* 2007;13:254–6.
 155. Akita K, Sakaguchi-Kuma T, Fukino K, Ono T. Masticatory muscles and branches of mandibular nerve: positional relationships between various muscle bundles and their innervating branches. *Anat Record (Hoboken).* 2019;302:609–19.
 156. McDonald MH, Hoffman MR, Gentry LR, Jiang JJ. New insights into mechanism of Eustachian tube ventilation based on cine computed tomography images. *Eur Arch Otorhinolaryngol.* 2012;269:1901–7.
 157. Manoharan SM, Gray R, Hamilton J, Mason MJ. Internal vascular channel architecture in human auditory ossicles. *J Anat.* 2022;241:245–58.
 158. Kamrava B, Roehm PC. Systematic review of ossicular chain anatomy: strategic planning for development of novel middle ear prostheses. *Otolaryngol Head Neck Surg.* 2017;157:190–200.

159. De Greef D, Goyens J, Pintelon I, Bogers JP, Van Rompaey V, Hamans E, Van de Heyning P, Dirckx JJJ. On the connection between the tympanic membrane and the malleus. *Hear Res.* 2016;340:50–9.
160. Gan RZ, Sun Q, Dyer RK, Chang K-H, Dormer KJ. Three-dimensional modeling of middle ear biomechanics and its applications. *Otol Neurotol.* 2002;23:271–80.
161. Sim JH, Puria S. Soft tissue morphometry of the malleus–Incus complex from micro-CT imaging. *J Assoc Res Otolaryngol.* 2008;9:5.
162. Graboyes EM, Hullar TE, Chole RA. The lenticular process of the incus. *Otol Neurotol.* 2011;32:1600–4.
163. Chien W, Northrop C, Levine S, Pilch BZ, Peake WT, Rosowski JJ, Merchant SN. Anatomy of the distal incus in humans. *J Assoc Res Otolaryngol.* 2009;10:485–96.
164. Enghag S, Strömbäck K, Li H, Rohani SA, Ladak HM, Rask-Andersen H, Agrawal S. Incus necrosis and blood supply: a micro-CT and synchrotron imaging study. *Otol Neurotol.* 2019;40:e713–22.
165. Bolz EA, Lim DJ. Morphology of the stapediovestibular joint. *Acta Otolaryngol.* 1972;73:10–7.
166. Sim JH, Rööslä C, Chatzimichalis M, Eiber A, Huber AM. Characterization of stapes anatomy: investigation of human and guinea pig. *J Assoc Res Otolaryngol.* 2013;14:159–73.
167. Guggenheim P. Mesenchyme in the middle ear. *Laryngoscope.* 1971;81:1665–70.
168. Marquet J. The incudo-malleal joint. *J Laryngol Otol.* 1981;95:543–65.
169. Mason MJ, Farr MRB. Flexibility within the middle ears of vertebrates. *J Laryngol Otol.* 2013;127:2–14.
170. Kierner AC, Mayer R, v Kirschhofer, K. Do the tensor tympani and tensor veli palatini muscles of man form a functional unit? A histochemical investigation of their putative connections. *Hear Res.* 2002;165:48–52.
171. Ramirez Aristeguieta LM, Ballesteros Acuña LE, Sandoval Ortiz GP. Tensor veli palatini and tensor tympani muscles: anatomical, functional and symptomatic links. *Acta Otorrinolaringol Espanola.* 2010;61:26–33.
172. Howell P. Are two muscles needed for the normal functioning of the mammalian middle ear? *Acta Otolaryngol.* 1984;98:204–7.
173. Jones SE, Mason MJ, Sunkaraneni VS, Baguley DM. The effect of auditory stimulation on the tensor tympani in patients following stapedectomy. *Acta Otolaryngol.* 2008;128:250–4.
174. Pang XD, Peake WT. *How* do contractions of the stapedius muscle alter the acoustic properties of the ear? In: Allen JB, Hall JL, Hubbard A, Neely ST, Tubis A, editors. *Peripheral auditory mechanisms.* New York: Springer; 1986. p. 36–43.
175. Mukerji S, Windsor AM, Lee DJ. Auditory brainstem circuits that mediate the middle ear muscle reflex. *Trends Amplif.* 2010;14:170–91.
176. McManus LJ, Dawes PJ, Stringer MD. Clinical anatomy of the chorda tympani: a systematic review. *J Laryngol Otol.* 2011;125:1101–8.
177. Monkhouse WS. The anatomy of the facial nerve. *Ear Nose Throat J.* 1990;69:677–83, 686–7.
178. Shin KJ, Gil YC, Lee JY, Kim JN, Song WC, Koh KS. Three-dimensional study of the facial canal using microcomputed tomography for improved anatomical comprehension. *Anat Record (Hoboken).* 2014;297:1808–16.
179. Ito J, Oyagi S, Honjo I. Autonomic innervations in the middle ear and pharynx. *Acta Otolaryngol Suppl.* 1993;506:90–3.
180. Eden AR, Gannon PJ. Neural control of middle ear aeration. *Arch Otolaryngol Head Neck Surg.* 1987;113:133–7.
181. Songu M, Aslan A, Unlu HH, Celik O. Neural control of eustachian tube function. *Laryngoscope.* 2009;119:1198–202.
182. Kanzara T, Hall A, Virk JS, Leung B, Singh A. Clinical anatomy of the tympanic nerve: a review. *World J Otorhinolaryngol.* 2014;4:17–22.
183. Ross JA. The function of the tympanic plexus as related to Frey's syndrome. *Laryngoscope.* 1970;80:1816–33.
184. Padurariu S, Rööslä C, Røge R, Stensballe A, Vyberg M, Huber A, Gaihede M. On the functional compartmentalization of the normal middle ear. Morpho-histological modelling parameters of its mucosa. *Hear Res.* 2019;378:176–84.
185. Cros O, Knutsson H, Andersson M, Pawels E, Borga M, Gaihede M. Determination of the mastoid surface area and volume based on micro-CT scanning of human temporal bones. Geometrical parameters depend on scanning resolutions. *Hear Res.* 2016;340:127–34.
186. Singh A, Thakur R, Kumar R, Verma H, Irugu DVK. Grading of the position of the mastoid tegmen in human temporal bones—a surgeon's perspective. *J Int Adv Otol.* 2020;16:63–6.
187. Louis RG Jr, Loukas M, Wartmann CT, Tubbs RS, Apaydin N, Gupta AA, Spentzouris G, Ysique JR. Clinical anatomy of the mastoid and occipital emissary veins in a large series. *Surg Radiol Anat.* 2009;31:139–44.
188. Ozer E, Bayazit YA, Kara C, Mumbaç S, Kanlikama M, Gümüşburun E. Körner's septum (petrosquamosal lamina) and chronic ear disease. *Surg Radiol Anat.* 2004;26:118–21.
189. MacEwen W. Pyogenic and infective diseases of the brain and spinal cord: meningitis, abscess of brain, infective sinus thrombosis. *Glasgow Med J.* 1893;41:57–63.
190. Doyle WJ. The mastoid as a functional rate-limiter of middle ear pressure change. *Int J Pediatr Otorhinolaryngol.* 2007;71:393–402.
191. Gaihede M, Dirckx JJ, Jacobsen H, Aernouts J, Søvsø M, Tveterås K. Middle ear pressure regulation—complementary active actions of the mastoid and the Eustachian tube. *Otol Neurotol.* 2010;31:603–11.
192. Cinamon U, Sadé J. Mastoid and tympanic membrane as pressure buffers: a quantitative study in a middle ear cleft model. *Otol Neurotol.* 2003;24:839–42.
193. Takahashi H, Honjo I, Naito Y, Miura M, Tanabe M, Hasebe S, Toda H. Gas exchange function through the mastoid mucosa in ears after surgery. *Laryngoscope.* 1997;107:1117–21.
194. Belyea J, Wickens B, Bance M. Middle ear ventilation status post-operatively after translabyrinthine resection of vestibular schwannoma with mastoid obliteration and Eustachian tube occlusion: is the Eustachian tube enough to ventilate the middle ear without the mastoid air cell system? *J Otolaryngol Head Neck Surg.* 2016;45:44.
195. Swarts JD, Cullen Doyle BM, Alper CM, Doyle WJ. Surface area-volume relationships for the mastoid air cell system and tympanum in adult humans: implications for mastoid function. *Acta Otolaryngol.* 2010;130:1230–6.
196. Stepp CE, Voss SE. Acoustics of the human middle-ear air space. *J Acoust Soc Am.* 2005;118:861–71.
197. Magnuson B. Functions of the mastoid cell system: auto-regulation of temperature and gas pressure. *J Laryngol Otol.* 2003;117:99–103.
198. Ilea A, Butnaru A, Sfrângeu SA, Hedeşiu M, Dudescu CM, Berce P, Chezan H, Hurubeanu L, Trombiţaş VE, Câmpian RS, Albu S. Role of mastoid pneumatization in temporal bone fractures. *AJNR Am J Neuroradiol.* 2014;35:1398–404.
199. Proetz AW. Observations upon the formation and function of the accessory nasal sinuses and the mastoid cells. *Ann Otol Rhinol Laryngol.* 1922;31:1083–99.
200. Alicandri-Ciuffelli M, Gioacchini FM, Marchioni D, Genovese E, Monzani D, Presutti L. Mastoid: a vestigial function in humans? *Med Hypotheses.* 2012;78:364–6.